7-3-2018

Modeling and Analysis of Thermal Effects on A Fractured Wellbore During Lost Circulation and Wellbore Strengthening Processes

Ze Wang
Louisiana State University and Agricultural and Mechanical College

MODELING AND ANALYSIS OF THERMAL EFFECTS ON A FRACTURED WELLBORE DURING LOST CIRCULATION AND WELLBORE STRENGTHENING PROCESSES

A Thesis

Submitted to the Graduate Faculty of the
Louisiana State University and
Agricultural and Mechanical College
in partial fulfillment of the
requirements for the degree of
Master of Science in Petroleum Engineering

in

The Department of Petroleum Engineering

by
Ze Wang
B.S., China University of Petroleum (Beijing), 2015
August 2018

Acknowledgments

This thesis is built up based on the simulations and experimental works I have been working on for the last two years. I won't be able to complete my research without the valuable instruction of my major advisor, Prof. Yuanhang Chen. Dr. Chen offered both general methodologies and specific knowledge that prove to be essential support during my whole academic study. When it comes to obstacles that seem difficult to overcome, he was always willing to offer precious life lessons that motivate us through challenging tasks. His attitude and determination will be constant inspirations in my future path to go.

I also want to thank my committee member and our graduate advisor Prof. Andrew K. Wojtanowicz. Prof. Wojtanowicz is the most conscientious advisor and experienced professor I have ever met. He encourages us to research in a way that agrees to the physical logic and engineering practice, which I believe is the true essence of engineering study. Though harsh and rigid, he can always make a conversation interesting and thought-provoking by his great knowledge and humor.

Prof. Shengli Chen, who is an expert in the are of my study, also kindly shared his wisdom and provided useful suggestions to help me complete my thesis

I want to express deep appreciation to my parents, which is the fundamental reason of my existence. Through disagreements and fights, there might be, they are always on my side no matter what happened. Every step of my life, good or bad, won't be complete without their love and encouragements.

My friends here, they are amazing. Their spirits to enjoy the moment and confront life choices impacted my way of living and thinking in many different ways. My life here in LSU was such a wonderful adventure and fun exploration only because of them.

Table of Contents

List of Symbols

α_T : Thermal expansion coefficient.

α: Biot constant.

σ: Stress tensors

C_p: Heat capacity at constant pressure

C_r : Rock specific heat (Heat capacity)

C: Elastic tensor

ε: Strain tensors

ε_T : Thermal strain

ε_v : Volumetric strain

E: Young's modulus

Φ: Rock Porosity

K: Rock Permeability

K_{eq}: Equivalent thermal conductivity of the solid-liquid system

K_r : Rock thermal conductivity

L: Model length

L_f : Fracture length

ρ: Density

$(\rho C_p)_{eq}$: The equivalent volumetric heat capacity of the solid-liquid system.

μ: Fluid viscosity

ν: Poisson's ratio

p_f: pore pressure

p_{pore} : Initial pore pressure

p_w: Wellbore pressure

Q: Heat source

Q_f: Fluid source in/out of certain porous space

Q_m : Mass source in/out of porous space

q : Darcy velocity field

ρ_r : Rock density

ρ_r : Drilling fluid density

R_w: Wellbore radius

s_0, s: original and changed stress state of porous media

S_{hmin} : Minimum horizontal stress

S_{hmax} : Maximum horizontal stress

$T - T_{ref}$, temperature increase/decrease in the rock matrix.

T_r : Initial reservoir temperature

T_{wf}: Wellbore temperature

u : Velocity field of fluid flow in porous media

v_{in} : Fluid leak-off rate

Abstract

To successfully prevent fracture propagation and combat lost circulation, a thorough understanding of the stress state in the near-wellbore region with fractures is imperative. One important factor that is not yet fully understood is how temperature variation during lost circulation affects pre-existing or newly initiated fractures. To address this problem, a 3D finite element analysis was conducted in this study to simulate the transport processes and state of stresses in the near-wellbore region during mud invasion into fractures. To take the thermal effects into account, a thermo-poro-elasticity model was coupled with flow and heat transfer processes. This study included a series of sensitivity analyses based on different formation properties and mud loss conditions to delineate the relative importance of different parameters on induced thermal stresses. The results demonstrate how the stresses redistribute as non-isothermal mud invasion takes place in fractures. They show that a temperature difference between the formation rock and the circulating muds can facilitate fracture propagation during mud invasion. The thermal effect can also diminish the enhanced hoop stress, which is the tangential stress acts to close the fracture, provided by Wellbore Strengthening and other lost circulation prevention methods. Such information is important to successful management of lost circulation by taking into account thermal effects from different lost circulation prevention approaches. The conclusions of this study are particularly relevant when a large temperature difference exists between circulating fluids and surrounding rock as commonly seen in high-pressure high temperature (HPHT) and deepwater wells.

Chapter 1. Introduction

A severe lost circulation event is usually associated with the emanation and propagation of pre-existing or drilling induced fractures from oil/gas wells. During drilling operations, one of the essential tasks is to maintain hydraulic pressure caused by mud volume in the wellbore between appropriate pressure windows. The high fluid pressure in the wellbore can sustain pore pressure in underground formations, like an aquifer, and support the wellbore wall to keep it from collapse in. The collapse pressure or pore pressure decides the lower boundary of the mud weight. On the other hand, if the downhole hydraulic pressure exceeds the tensile strength of formation rock, formation rock will break and fractures can occur and start to propagate from the wellbore wall. Downhole fluid pressure at this point is called fracture pressure. Fractures emanating from the wellbore wall provide a convenient channel for the mud to escape into the near wellbore region.

Lost circulations events can be especially threatening when drilling into formations with abnormal pressure distribution. Drilling operations can be another reason for pressure fluctuation in a wellbore. Swab or trip in/out of drill pipe can also cause abnormal pressure surges in a wellbore and increase pressure until fracture pressure is exceeded. Lost circulation has been identified as one of the major causes of non-productive time (NPT) and an increase of drilling cost.

To combat lost circulation problems, the primary considerations are to clog fluid loss channel and prevent fractures from further propagation. Lost circulation materials (LCM) such as particle and fibrous materials are wildly applied to seal the fluid loss channel and mitigate lost circulation events. Among the wild selection of LCM, one category is carefully engineered particle materials that aim to bridge fractures and protect fractures from further initiation and propagation and strengthen the pressure-bearing capacity of the wellbore. The implementations of these well-engineered materials are called wellbore strengthening (WBS) and the carefully designed particles

are sometimes referred more specifically as wellbore strengthening materials (WSM). Most common WBS involves using lost circulation materials (LCM) in drilling fluid to prop, bridge, or seal the fractures by use of particle additives. During last decade, successful WBS operations have been reported in many drill sites. Regretfully, there is still no consensus on the fundamental mechanisms to explain how WBS works.

Regarding stress state of underground formation rocks during WBS, the effect of temperature and thermal stress is an indispensable parameter that is usually neglected in the study of WBS. Due to the geothermal gradient, formations or reservoirs at the location thousands of feet underground bear much higher temperature than the temperature at the surface. During circulation of drilling fluid within the wellbore, fluid is gradually heated up and the surrounding hot rocks are cooled down at the bottom of the wellbore. Though wellbore heating is possible when drilling into frozen formations or at a shallow section of the wellbore, it is goes beyond the discussion of this study. While formation cooling takes place, thermal contraction of formation rock can induce significant thermal stresses around the wellbore. The thermal effect has been well recognized in the previous studies about the stress state and stability of an intact wellbore. Many researchers have also obtained numerical and analytical solutions for the fracture pressure under the thermal effect. Analytical solutions barely consider the thermal effect or pore pressure due to a lack of theoretical background in such problems. Numerical solutions face difficulties in doing so mainly because of the complexity of coupling heat transfer with pore pressure and poroelasticity in the near wellbore formation.

This thesis uses finite element analysis to simulate the thermally induced stress around a wellbore using a 3D fully coupled thermo-poro-elasticity model. Heat transfer between the wellbore fluid and formation was coupled with pore fluid flow in a porous medium to generate a

temperature field in the near-wellbore region. Both heat convection dominated by fluid leak-off and heat conduction within the rock matrix were considered in this process. The thermal expansion coefficient of the rock matrix and the thermal stress it caused was incorporated into the poroelasticity model to demonstrate how the stress changed as the formation's temperature was affected by the cold mud invasion. We were able to show how much the temperature can impact the formation through stress analysis of the wellbore and fracture tip, and how it relates to the hoop stress.

Another particular goal of this work is to discuss how convective and conductive heat transfer during lost circulation affects the hoop stress of a wellbore with pre-existing or induced fractures. The findings of this study will be beneficial to evaluate the risk of re-initiating fractures from a wellbore due to a significant change in the temperature of the formation. Furthermore, based on these findings, important recommendations were suggested to help determine proper fracture gradients and wellbore pressures in various field operations.

This study includes four major chapters other than the introduction. The second chapter reviews previous studies regarding the thermal effect on wellbore stability and fracture initiation. The third chapter presents the methodology and boundary conditions to simulate the local stress state under wellbore cooling. Chapter four display results from case studies to discuss the application of this model in different scenarios such as lost circulation and WBS. At last, Chapter five discusses the variation of wellbore temperature due to the fluid additives.

Chapter 2. Literature Review

Lost circulation has been identified as one of the major causes of NPT and increase of drilling cost (Cook et al., 2011, Carpenter et al. 2014). A certain amount of mud can be sacrificed during slightly lost circulations to continue the drilling process before wellbore is cemented and casings are implemented. But when a severe lost circulation event occurs, the operation has to be stopped. Reports showed that 12% of the non-productive time in shelf drilling of Gulf Mexico was related to lost circulation events. There're also reports showing that lost circulation events were responsible to 10% to 20 % of the cost during the whole drilling circle (Growcock, 2009).

To combat lost circulation problems, the primary considerations are to clog fluid loss channel and prevent fractures from further propagation. Wellbore strengthening (WBS) refers to a collection of techniques applied to serve such purposes by strengthening the pressure-bearing capacity of the wellbore. Wellbore strengthening techniques are categorized into preventative and remedial approaches depending on whether they are applied before or after a fluid loss is detected (Feng, 2017). Preventative approaches raise the fracture pressure of the formation being drilled by facilitating the establishment of a filter cake on the wellbore wall. Functions of filter cake are twofold. Filter cake usually has low permeability and high ductility. By forming this low permeable layer on wellbore wall, pressure communication from the wellbore to formation porous media is interrupted. Thus, the negative impact of high wellbore pressure or abnormally low pore pressure is mitigated by the isolation effect of the filter cake. Meanwhile, filter cake also helps to plastering the micro fracks or pre-existing natural fractures on wellbore wall. Our emphasis of study is remedial approaches that are applied after lost circulations occur and fractures are identified.

Most common remedial WBS involves using LCMs in drilling fluid to prop, bridge, or seal the fractures by use of lost circulation materials in drilling fluid. (Feng, 2016). The initial concept of

strengthening the wellbore mechanically was first brought up decades ago. When researchers creatively applied particle materials with a range of sizes into drilling fluid, they found out that lost circulation can be mitigated effectively (Fuh et al, 1992). During last decade, successful WBS operations have been reported in many drill sites. But regretfully there is still no consensus on the fundamental mechanisms to explain how WBS works. WBS techniques are generally theorized to work by either of the three mechanisms (Alberty et al., 2004, Saeed, 2012, van Oort et al.,2011, Mehrabian et al., 2015, Feng et al., 2017).

(a) Stress cage: LCM prop and widen the near wellbore fractures open against the in-situ stress and develop a sufficient supplementary hoop stress around the wellbore to considerably increase its fracturing limit. For stress cage theory to work, it's of the highest priority to engineer the LCM so the it has sufficient strength and proper size to fit in the fracture and support the fracture wall perfectly. It also requires formation to have high hardness so the particles materials are not embedding into the formation. This explanation is limited due to its demanding requirements to be effective.

(b) Fracture closure pressure: LCM type is not of prime consideration for this hypothesis to take effect. Instead, it is aimed to deposit LCM materials at some distance inside the fracture, while clogging the fracture and maintaining enough fracture width and allows fluid to increase its closure pressure. The essential mechanism of this hypothesis also includes isolating fracture tip from high fluid pressure in the wellbore by allowing fluid in fracture beyond fracture bridge to leak off into formation, as showed in the Figure 2.1.b) The fluid trapped behind the plug diffuses into the pore space of surrounding rocks, leaving the fracture tip with significant reduced pressure. The reduced pressure will make the fracture less likely to propagate farther into the formation. High fluid loss, and consequently a permeable formation, is important to the success of this method. Carefully

designed particle size distribution (PSD) of LCM plays the key role to create impermeable bridging inside the fracture.

(c) Fracture propagation resistance (FPR): FPR theory is proposed most commonly in oil-based mud (OBM) and synthetic-based mud (SBM). Likewise, it is reliant on the tip-isolation concept, but does not require high fluid loss. Contrary to the fracture bridging and plugging, pressure communication from wellbore to fracture tip is not interrupted in FPR. Fracture tip in FPR is protected in this case by generating a thin layer of filter cake along fracture surface and cover fracture tip. The build-up inner filter cake changed the permeability distribution around fractures and restricts fluid invasion through the fracture tip. Theoretically it could also keep fracture tip from the impact of high fluid loss. Meanwhile, particle materials accumulated around fracture tip also provided certain degree of mechanical strength and resist the fracture from fracture propagation.

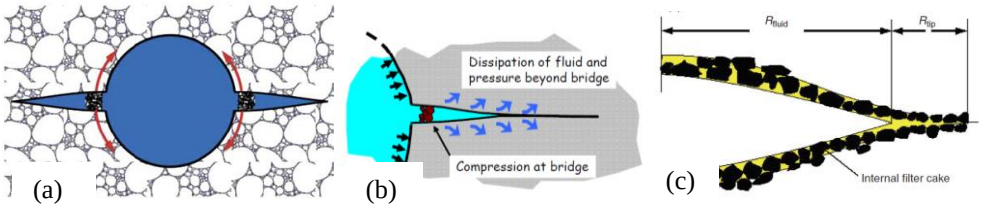

Figure 2.1. Three different mechanism to explain WBS: (a) stress cage (Mehrahian et al., 2015) (b) fracture closure pressure (c) fracture propagation resistance (Morita et al., 1990, van Oort, 2011).

In WBS practice during drilling, either of the three mechanisms mentioned above could be the major drive behind the increased wellbore fracture gradient, or they could have combined effects. For example, the plug inside the fracture could increase the hoop stress around wellbore while at the same time isolating the fracture tip. In porous media, stress state is affected by pore pressure. As shown previously, fracture plugging not only provide hoop stress enhancement around the wellbore, it also restricts fluid flow into fractures during lost circulation and alter pore pressure

and therefore stress state around the fracture.

Based on these mechanisms, several important analytical studies are proposed to study the WBS effect. These studies try to determine fracture pressure and fracture geometry when WBS is applied. Earlier researchers extend the concept of the penny-shaped fractures from hydraulic fracturing to study the effect of LCMs on near wellbore fractures (Ito et al., 2001). In their study, the effect of LCMs on fracture pressure was determined when particle materials located in different locations inside the fracture. They assumed relatively long fractures so the wellbore can be ignored. This becomes a shortcoming of their studies for they failed to consider the state of the wellbore during WBS operations. Their studies are also not applicable when fractures are short, which is the most common case in lost circulation.

By linear elastic fracture mechanics and principles of superposition, later researchers proposed other analytical solutions (Guo et al., 2011; Morita 2012; Shahri et al., 2014; Feng et al, 2016). Most of these studies adopted a wellbore with two short fractures emanating from the wellbore symmetrically. These studies developed appropriate solutions to calculate the fracture width and fracture pressure before and after the fractures are plugged by LCMs. They have also investigated some major parameters that affect the performance of LCMs like Young's Modulus, wellbore size, and in-situ stresses. These models are already very comprehensive by involving more realistic fracture geometry and drilling parameters. However, they still didn't take pore pressure into consideration because of the linear elasticity theory they were based on. Meanwhile, their studies also consider a perfect bridge meaning that fluid invasion into fractures is completely prevented by the particle materials, which is also very rare in real life situation.

In previous studies to assess the effectiveness of lost circulation prevention methods, many indispensable factors were neglected to simplify the proposed models, one of them is the thermal

effect due to the invasion of mud with a temperature different from that of the surrounding rocks.

The extent to which the relatively cold drilling fluids affect the warm formations is now being recognized as having a significant effect on the wellbore's fracture gradient. Analysis of field data from deep-water wells shows that lost circulation events are closely associated with a significant variation between the formation temperature and fluid temperature during drilling (Chen et al. 2015 & 2016, Hettema et al., 2004, Pepin., 2004). To investigate the effect of fluid temperature on wellbore fracturing, leak-off tests conducted in South Texas also emphasized a reduced fracture gradient as a result of this temperature drop (Gonzalez et al., 2004). A simplified solution of the wellbore fracture gradient under thermal effect while drilling was also proposed in this study by assuming a pure thermoelasticity without considering the pore pressure.

Further studies emphasizing the thermal effect during drilling provided comprehensive analytical solutions to the wellbore stress state under cooling or heating processes. Their studies managed to consider pore pressure and pore fluid flow when calculating near wellbore temperature and thermal stress redistribution (Chen et al., 2005, Fjær et al., 2008, Maury et al., 1995, Yan et al., 2013). Furthermore, they offered important references for the determination of fracture and collapse pressure of an intact wellbore under the thermal effect. In these previous studies, the effect of pre-existing or induced fractures is usually not considered when predicting the fracture gradient. However, in practice, severe losses occur not just from fracturing a perfect wellbore, but also from a re-initiation of pre-existing fractures from the wellbore.

Previous studies on fracturing behavior mainly investigated such effects by considering hot, dry reservoirs (Maury, 1995, Zhou et al., 2010). A study has been conducted in hydraulic fracturing to analyze fracture initiation and propagation (Rinne, 2012). This study only illustrated the fracture propagation behavior under particular mechanical and thermal loading. A detailed analysis of how

stress distribution around the fractured zone reacts to temperature change was not specified. Moreover, these studies fail to give sufficient consideration to different lost circulation prevention or WBS scenarios.

The success of current methods used to prevent lost circulation has been strongly related to the elevation of hoop stress, the stress acting to close the fracture, in the near-wellbore region. When there is a large temperature gradient between the fluid and the formation, the hoop stress decreases, allowing a fracture to propagate. A consequence of reducing the hoop stress is that WBS and other lost prevention methods will perform less effectively than they are expected to. By far, the extent to which the thermal effect on lost circulation events and mitigation methods during drilling is not well understood and quantified yet, especially in the context of an imperfect wellbore.

Chapter 3. Problem Definition and Important Assumptions

3.1 Problem definition and scope of work

The problem is defined in this section followed by a generally explained methodology. This work mainly discusses the effect of temperature change on a fractured wellbore when drilling fluid lost into the formation. Study of temperature and stress variation during lost circulation inevitably involves the coupling of multiple physical processes. Heat transfer and temperature change in near wellbore area are controlled by the fluid flow in porous media induced by fluid invasion. This process generated thermal stress and altered the stress state of rock matrix in near wellbore region. Such stress redistribution leads to the change of pore space volume and pore pressure, thus influence the fluid flow through the matrix, conversely.

The following graph in Figure 3.1. shows the simplified 2D representation of the 3D model established in this study, which is characterized by a circular wellbore and pre-existing fractures. The geometry describes an intersection of a vertical wellbore that subjects to a minimum and maximum horizontal stress from X and Y direction. Two short fractures are pre-set symmetrically on the wellbore perpendicular to minimum horizontal stress.

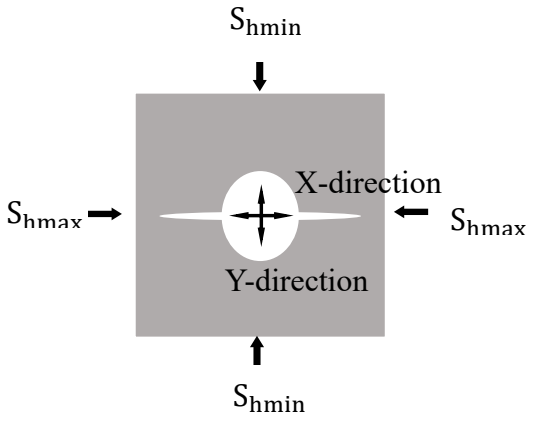

Figure 3.1. Simplified 2D representation of the 3D model established in this study

This study uses the law of Darcy's flow to control the fluid flow and pore pressure distribution in the rock matrix. To simulate fluid loss through fractures, fluid inlet is set up on both wellbore wall and fracture surface. Together with the fluid pressure exerted on the outer boundary, fluid inlet setting could control the pore pressure distribution, as well as the convective heat exchange through fluid inflow. In-situ stresses and fluid pressure on wellbore wall and fracture surface contribute to the mechanical balance of this model. The fluid pressure that supports the fractures would be higher than minimum horizontal stress to maintain the fractures in a certain width.

Follow the natural path from theoretical study to practical application, this thesis categorizes the scope of work in two part: a) study the stress state of a fractured wellbore during the cooling process of formation due to fluid invasion; b) explore the possibility of using improved drilling fluid to protect the formation rock surrounding the wellbore from stress variation due to the decline of temperature.

The first part of the study aimed to answer how does stress variation around wellbore due to formation cooling would affect fracture re-initiation. A large quantity of fluid loss into the formation through induced fractures is one major problem during drilling. Further development of fracture due to thermal stress could deteriorate the situation and counteract the efforts to mitigate fluid loss. This thesis uses finite element method to simulate stress field around a fractured wellbore with lost circulation implementation, given its inherent capability and convenience to adopt complicated geometries. Many factors would be involved when discussing fluid invasion and induced thermal stress. Parametric studies and statistical techniques are adopted to discover their individual effect and relative importance. Then, most importantly, WBS component is implemented into the numerical modeling to determine how much WBS should be weakened by

the formation cooling.

The second part of this study explores the potential of wellbore temperature control by manipulating the thermal properties drilling fluid. Changing the heat transfer process in the wellbore is extremely difficult. Efforts to reduce or increase wellbore temperature are strongly limited by complicated downhole requirement such as wellbore size, wellbore pressure window, equipment temperature range, circulating fluid properties, economic reasons and so on. This study proposes to use special additives into drilling fluid to mitigate the heat exchange between wellbore fluid and surrounding formations. There are two ways for these additives to intercept the heat transmission process in the wellbore. Adding thermal insulating materials could reduce the thermal conductivity of the drilling fluid and affect heat exchange between circulating fluid and formation rock. These additives could also potentially be helpful to protect formation from heat loss by altering the composition of the filter cake that covers a certain section of the wellbore. Models and methods to evaluate the effect of these additives will be given in detail in the chapter of Methodology.

3.2 Important assumptions

This study investigates how the near wellbore stress around a fractured zone will react as the formation's temperature drops. The following assumptions are made in the modeling of a fractured wellbore.

- Isotropic and homogeneous formation rock is assumed in this thesis for the simplification of the modeling.
- The modeling assumes a circular-shaped vertical wellbore with two short fractures generates perpendicular to the minimum horizontal stress.
- This thesis assumes that the formation rock has sufficient tensile strength that prevents the

pre-existing fracture from further propagation. Failure criteria of formation rock at fracture tip and fracture propagation are not considered in the modelling.

- Uniform pressure and temperature values are pre-set on wellbore and fracture surface in the fluid invaded zone. The limitation of FEM software unable the simulation of fluid and heat flow inside void space of fracture. When fluid invasion happens through fracture surface, the temperature and pressure gradient along the short distance from fracture mouth to fracture tip would be negligible. This justified using uniform fluid and temperature boundary to be an effective supplement of fluid and heat flow inside fracture during lost circulation.

Chapter 4. Theoretical Background

Chapter 4 covers the fundamental theories underlying the study in this thesis. Some important terminologies useful to later discussions are also introduced in this chapter. The first part of this section reviews the basic concepts in linear elasticity and introduces the stress state around a perfect wellbore. Part one also covers the thermal effect on stress state around wellbore with consideration of linear elasticity and poroelasticity. Then in the second part, fundamentals of fracture mechanics are introduced, and basic theories of stress intensity factor (SIF) is built, including the extension of fracture mechanics in wellbore breakdown. The last part of theory background explains fundamental equations that control the stress redistribution around a fractured wellbore during drilling fluid invasion. These equations adopted in the finite element study presents coupling nature of this multi-physic process of thermoporoelasticity.

4.1 Basics of linear elasticity: stress surround wellbore and effect of thermoelasticity.

4.1.1 Stress and strain

Elasticity is the ability of a material to recover to the initial state after the deformation caused by external forces. In the simplest case, the external forces are related to the consequential deformation of materials in a linear way, which called linear elasticity. When the forces and deformation are infinitely small, most of the solid materials present a linear elasticity. Thus linear elasticity is the foundation of all other elasticity and non-elasticity studies.

4.1.2 Rock stresses surround a wellbore

Drilling into underground formation requires a thorough understanding of its mechanical behavior, present stress state and the geological structure creating the stress. This initial stress state of a geological point underground is called in-situ stress, as showed in Figure 4.1. From a rock mechanic point of view, in situ stress is a major factor to maintain the mechanical stability of a

drilled wellbore. In situ stress also dominate the initiation and development of fractures. In the convention of rock mechanics study, a rock block is assumed to bear three principle stresses, orthogonal to each other. The direction of principle stresses is organized so that they act purely to compress the rock block without any shearing. Direction and magnitude of principle stresses vary depending on the depth of the rock, materials, and structure of overlying formation and special geological structures or activities such as fault, salt dome, erosion and tectonic movement. Commonly, vertical stress is assumed to be the maximum principle stress, and two horizontal stresses are intermediate and minimum principle stresses, as shown in Figure. The assumption is valid in a large range of depth and homogeneous earth materials, also when the block is not exposed to the stress from current or previous geological activities.

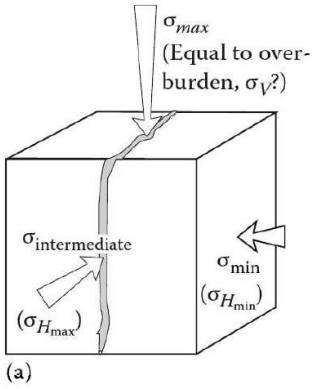

Figure 4.1. In-situ stress around a block of the underground earth (Smith et al. 2015)

Vertical stress comes from the weight of the overburden formation that the rock carries. It's convenient and reasonable to assume it as principle stress since it's caused by gravity and it acts vertically to the earth center. Consider a varying density of rock along a certain depth; vertical stress can be calculated by the following equation: $\sigma_v = \int_0^D \rho(z)gdz$, whereas D is the current

depth. Typical density measurement of overburden formation gives a value of 1 – 1.05 psi/ft or 0.0225 MPa/m of the gradient of vertical stress (Smith et al., 2015). Of course, offshore formation or abnormal pressurized zone will need extra corrections for water depths or extra pressure source. Horizontal stress can come from two sources: 1) overburden weight that compact formations and create horizontal stress; 2) tectonic forces from local geological activities. Based on the linear elasticity of rock and idea of uniaxial compaction, horizontal stress is expressed in $\sigma_h = \frac{\nu}{1-\nu}\sigma_v = K\sigma_v$, ν is Poisson's Ratio of rock and K can be treated like a rock parameter. For most rock materials, ν is closed to 0.25, which gives $\sigma_h = \frac{1}{3}\sigma_v$. This is a reasonable approximation of minimum horizontal stress in most cases.

The true stress act to compress the rock is not the total stress, but the net stress that takes into account the reservoir pore pressure. Fluid in overburden formation and connection to other fluid sources all contribute to the magnitude of pore pressure. Pore pressure acts normally on the inner surface of a porous rock saturated by reservoir fluid regardless of the direction. This introduced the idea of effective stress or Terzaghi's effective stress: $\sigma' = \sigma - p$ which expresses the relationship: effective stress = total stress – pore fluid pressure (Knappett et al., 2012). Plugging this into $\sigma'_h = K\sigma'_v$ gives: $\sigma_h - p = K(\sigma_v - p)$. Thus, the basic estimation of minimum horizontal stress can be written as and $\sigma_h = K(\sigma_v - p) + p$. In this equation, K is a rock property approximately equals 1/3, σ_v is overburden pressure with a gradient that usually varies from 1 - 1.05 psi/ft. p is the reservoir pressure.

The underground formation is constantly under a balanced compressive state due to overburden stress and tectonic forces. In mining or petroleum engineering, when a hole is drilling in a formation, a certain amount of solid is removed, and only fluid pressure inside will support the compacting forces from surrounding rock. When the fluid pressure inside does not provide the

equivalent stress as original earth, stresses around borehole wall, or wellbore wall in petroleum engineering, redistribute to regain the balance. If newly established stress state exceeds the failure criteria of the rock, the wellbore either collapse under compression or fractured under tension.

To study the stress state around the wellbore, it's more convenient to use the cylindrical coordinate system. In the cylindrical system, stress Consider a plane perpendicular to the z-axis, as showed in the Figure 4.2., stress in cylindrical coordination can be expressed by radial stress σ_r and tangential stress σ_θ in the following relationships (Salehi, 2012):

$$\sigma_r = \frac{1}{2}(\sigma_x + \sigma_y) + \frac{1}{2}(\sigma_x + \sigma_y)\cos 2\theta + \tau_{xy}\sin 2\theta \quad (4\text{-}1)$$

$$\sigma_\theta = \frac{1}{2}(\sigma_x + \sigma_y) - \frac{1}{2}(\sigma_x - \sigma_y)\cos 2\theta - \tau_{xy}\sin 2\theta \quad (4\text{-}2)$$

$$\sigma_z = \sigma_z \quad (4\text{-}3)$$

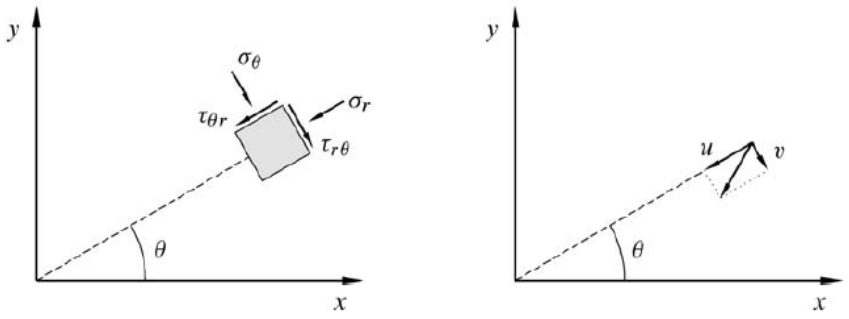

Figure 4.2. Rock stress in cylindrical coordinate. (Salehi, 2012)

The cylindrical expression of the stress state around a wellbore is illustrated in Figure 4.3. Under the linear elastic theory, the general solution of the stress state around a wellbore is first achieved by Kirsh in 1898 and then modified by others. Assuming a vertical wellbore and set $\sigma_{\theta 0}$ (stress at 0 degrees from X-axis) to be σ_h (horizontal stress perpendicular to X-axis) and consider the fluid pressure inside the wellbore p_w, stress around a circular wellbore can be expressed using following equations (Salehi, 2012):

$$\sigma_{rr} = \frac{\sigma_H - \sigma_h}{2}\left(1 - \frac{R_w^2}{r^2}\right) + \frac{(\sigma_H - \sigma_h)}{2}\left(1 + 3\frac{R_w^2}{r^2} - 4\frac{R_w^2}{r^2}\right)\cos 2\theta + \frac{R_w^2}{r^2}p_w \quad (4\text{-}4)$$

$$\sigma_{\theta\theta} = \frac{\sigma_H - \sigma_h}{2}\left(1 + \frac{R_w^2}{r^2}\right) - \frac{(\sigma_H - \sigma_h)}{2}\left(1 + 3\frac{R_w^2}{r^2}\right)\cos 2\theta + \frac{R_w^2}{r^2}p_w \quad (4\text{-}5)$$

$$\sigma_{zz} = \sigma_v - 2\nu(\sigma_H - \sigma_h)\frac{R_w^2}{r^2}\cos 2\theta \quad (4\text{-}6)$$

in which:

σ_{rr}, $\sigma_{\theta\theta}$ is the radial and tangential stress in cylindrical coordinate.

σ_H, σ_h are the horizontal stress perpendicular to Y-axis and X-axis, assume the minimum horizontal stress act perpendicular to X-axis.

p_w is the wellbore pressure or wellbore fluid pressure.

R_w is the wellbore radius

r is the radial distance from the point of interest to the center of the wellbore. ($r \geq R_w$)

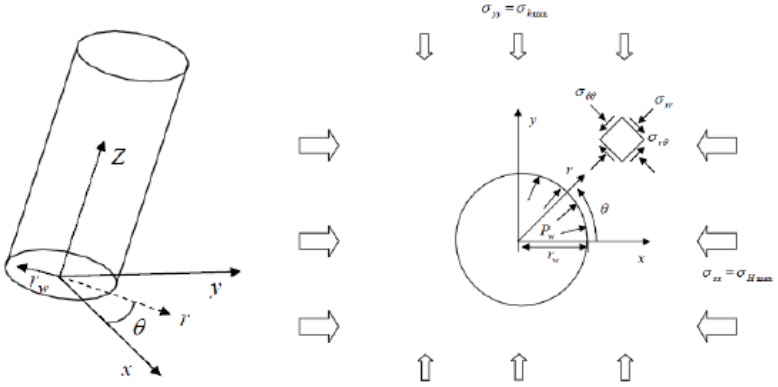

Figure 4.3. An arbitrarily oriented wellbore under in-situ stress system (Salehi 2012)

It is necessary to emphasize the concept of hoop stress. Here and in most cases in the following text, hoop stress is used more often to refer the tangential stress $\sigma_{\theta\theta}$. Hoop stress is named to express the compressive or tensile stress state at a point specifically in a cylindrical coordinate.

Wellbore stability is maintained by a highly compressive stress state offered by the overburden formation and weigh of drilling fluid or mud. In overbalance and underbalanced drilling, the mud weight that pressurizes the wellbore changes the hoop stress at wellbore wall. The wellbore will either fail in tension or collapse in compression when the hoop stress at wellbore wall exceeds the tensile or compressive strength of the rock. In this thesis, wellbore fracturing is more of interest. After the point of fracture initiation, hoop stress is still exerted perpendicular to fracture surface and counteract the width expansion of the fracture. It is so called closure pressure in many literatures regarding the induced fractures in drilling or hydraulic fracturing. Therefore, enhancement of hoop stress is a key to prevent initiation or further development of fractures resulting from a lost circulation event. At the wellbore wall, the equation above are reduced to:

$$\sigma_{rr} = p_w \tag{4-7}$$

$$\sigma_{\theta\theta} = \sigma_H + \sigma_h - 2(\sigma_H - \sigma_h)\cos 2\theta - p_w \tag{4-8}$$

$$\sigma_{zz} = \sigma_v - 2\nu(\sigma_H - \sigma_h)\cos 2\theta \tag{4-9}$$

This gives the minimum and maximum hoop stress along the wellbore at the direction of maximum and minimum horizontal stress, respectively, as showed in the Figure below.

$$\sigma_{\theta\theta min} = 3\sigma_h - \sigma_H - p_w \tag{4-10}$$

$$\sigma_{\theta\theta max} = 3\sigma_H - \sigma_h - p_w \tag{4-11}$$

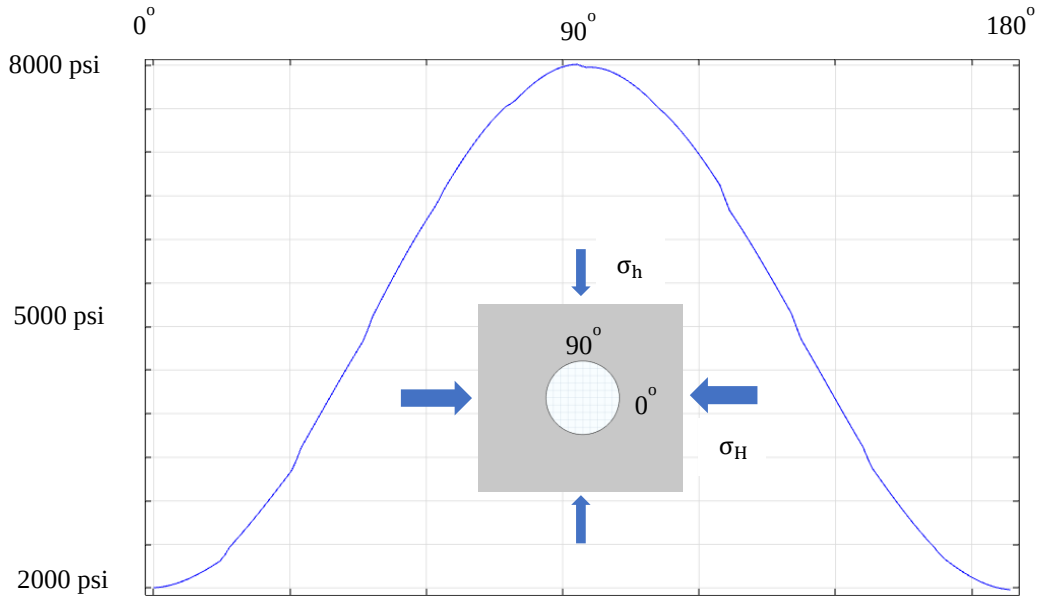

Figure 4.4. Maximum and minimum hoop stress along wellbore wall

4.1.3 Thermal effect and thermal stress

Thermal effect on wellbore, especially a fractured wellbore, is the primary task of this thesis. This problem results from the temperature difference between formation rock and reservoir fluid due to the geothermal gradient. In basic thermoelasticity, with the linearity of governing equations, thermal stresses can be combined with stress around the wellbore directly according to the superposition principle (Fjaer et al., 2008). Therefore, stress around wellbore wall can be modified as following equations:

$$\sigma_{rr} = p_w \tag{4-12}$$

$$\sigma_{\theta\theta} = \sigma_H + \sigma_h - 2(\sigma_H - \sigma_h)\cos 2\theta - p_w + \frac{E}{1-\nu}\alpha_T(T_{wf} - T_r) \tag{4-13}$$

$$\sigma_{zz} = \sigma_v - 2\nu(\sigma_H - \sigma_h)\cos 2\theta + \frac{E}{1-\nu}\alpha_T(T_{wf} - T_r) \tag{4-14}$$

In which,

E and ν are Young's Modulus and Poisson's ratio.

α_T is volumetric thermal expansion coefficient.

T_{wf}, T_r are the temperature in the wellbore and initial reservoir temperature.

These relationships only represent the thermal stress created only by conductive heat transfer in a simplest stationary process. However, the study of temperature change and thermal stress, in reality, should be conducted together with fluid flux and pore pressure in porous media of formation rock. The transient solution that couples the heat transfer with pore pressure and poroelasticity has been derived with the perfect wellbore.

4.2 Introduction of fracture mechanics in petroleum engineering.

Linear elastic fracture mechanics is fundamental to understand the basic fracturing behavior. Knowledge of materials fracturing start to build-up as early as the age of Renaissance, when Leonardo da Vinci started to investigate the cause underlying the fracturing of different materials (Salehi, 2012). Rock fracturing stems from an earlier study of other fragile materials like glass, metals, and ceramics. However, the inherent heterogeneity properties of formation rock and the complex anisotropy stress environment of underground formations all make the rock fracturing behave differently from other materials.

In ideal flat and sharp cracking, happening of fracture can be categorized into different modes according to the relative displacement of fracture surface and the strain type the fracture surfaces are subjects too, as showed in Figure 4.5. (Salehi, 2012).

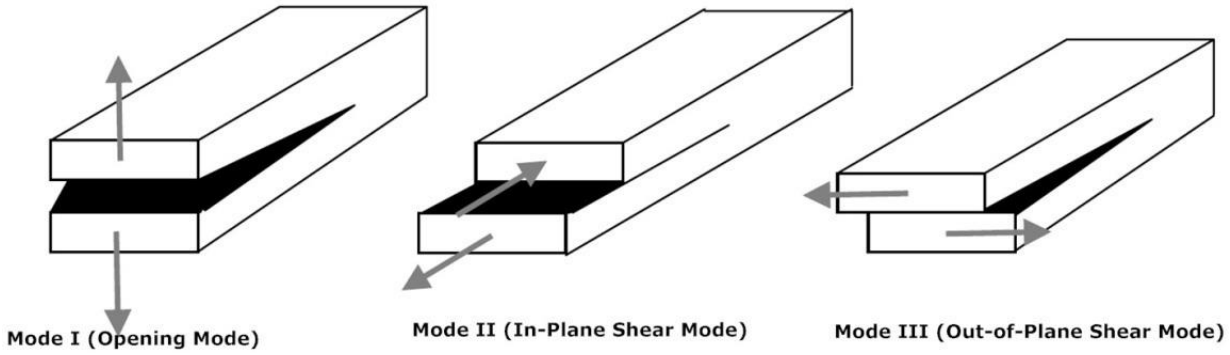

Figure 4.5. Fracture tip displacement mode. (Salehi, 2012)

As showed in Figure 4.5., Mode I is called opening mode for the reason that the fracture is created due to the normal stress exerted perpendicular to both of the fracture surfaces. Fracture tip is subjected to tensile failure in the opening mode. In Mode II, in-plane shearing fracturing, the shear stresses generate a fracture along the direction of shear stress. The fracture surfaces move or slide in the same plane relatively to each other. Mode III or out-of-plane shearing mode is the case when the direction of fracture propagation is perpendicular to the shear stresses.

Assuming vertical stress is the maximum principle stress, the fluid pressure in wellbore would first overcome the minimum horizontal stress and generate a fracture in the direction of maximum horizontal stress. Figure 4.6. shows the simplified intersection of a vertical wellbore that is fractured by the fluid pressure.

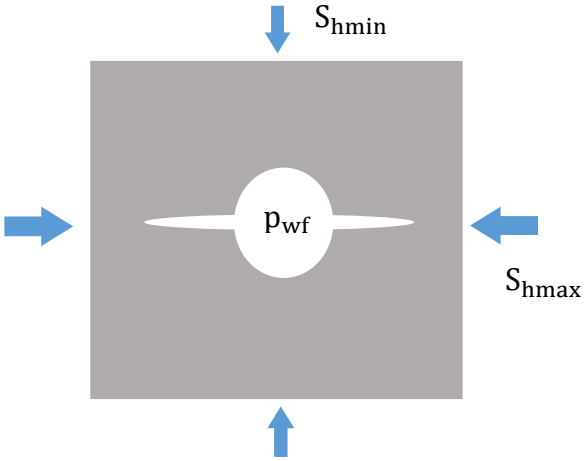

Figure 4.6. The intersection of a vertical wellbore with fracture generated perpendicular to the minimum horizontal stress.

For each of the fracturing mode, the energy required to initiate the fracture tip is different. In drilling or hydraulic fracturing, fractures in most cases are created in Mode I, in which the formation wall is rapture by high fluid pressure in the wellbore due to tensile failure. Griffith established the criteria for fracture initiation of material in as early as 1920. He formulated stress required to crack a material by considering materials properties and fracture shape. (Anderson, 1995)

$$\sigma_f = \left(\frac{\pi E \gamma_s}{2(1-\nu^2)a}\right)^{\frac{1}{2}} \tag{4-15}$$

With E and ν, this equation takes into account material mechanical properties. It also considers fracture shape by using "a" as fracture radius. γ_s in the equations refers to surface energy per unit. On the basis of this equation, Irwin (1954) gives the amount of energy needed for cracking to happen:

$$G = \frac{\pi\sigma^2 a}{E} \tag{4-16}$$

His equation is almost equivalent to the initial one but using energy release rate G at fracture tip to replace stress. Here, the criteria for the fracture to happen becomes $G = G_c$, in which Gc is the

critical energy release rate, also refers to fracture toughness. Gc is the critical strain energy release rate of a brittle material itself that indicates the resistance of the crack to further fracturing. In fracture mechanics, stress intensity factor (SIF) is used to refer to energy release rate for fracture under different fracture displace mode. K_I denotes the stress intensity factor under Mode I. K_I is related to strain energy release rate G with the equation $G = \frac{K_I^2}{E}$. What the SIF refers to critical strain energy Gc is usually referred to as fracture toughness, K_{IC}. SIF and fracture toughness is wildly adopted in fracture mechanics and petroleum engineering to evaluate the fracturing behavior. Measurement of fracture toughness, which is an inherent properties of the brittle materials, have been conducted extensively in previous studies (Clifton et al., 1976).

The stress intensity factor (SIF) is a commonly used concept in fracture mechanics caused by a remote load or residual stresses to predict the stress state ("stress intensity") near the tip of a crack. The magnitude of SIF depends on the geometry, size, location of the crack, and load distributions on the material and crack. According to the linear elasticity theory, a tensile fracture will start to extend when the value of the SIF approaches that of the fracture toughness K_{IC}.

Earlier equations for SIF mentioned in previous sections clearly cannot be applied for fractures with complicate geometry and loading conditions. Calculation of strain energy release rate is then developed into a path independent integral, denoted J, around the fracture tip in a two-dimensional elastic deformation problem (Dokhani et al., 2016, Feng et al. 2016, Rui et al., 2017), as shown in Equation 4-17. It can also be used as an approximation for simple three-dimensional problems with isotropic materials like in this study by selecting a cross section vertical to the wellbore.

$$G = J = \lim_{\Gamma \to 0} \int_{\Gamma} [W * n_1 - \sigma_{ij} n_j (\frac{\partial u_i}{\partial x_1})] ds \quad (4\text{-}17)$$

where W is the strain energy density of the material, σ_{ij} and u_i are the Cartesian components of the first stress tensor and displacement vector, respectively, n_j represents the Cartesian components of the outward unit vector normal to the contour Γ, and s is the arc length of the contour Γ, as is shown in Figure 4.7.

When the fracture face is subjected to surface traction, $\mathbf{t_c}$, integrations along C_1 and C_2 are included (Chang et al. 1992), that is,

$$J = \lim_{\Gamma \to 0} \int_{\Gamma} [W * n_1 - \sigma_{ij} n_j (\frac{\partial u_i}{\partial x_1})] ds - \int_{C_1} \left(\frac{\partial u_i}{\partial x_1}\right) ds - \int_{C_2} \left(\frac{\partial u_i}{\partial x_1}\right) ds \quad (4\text{-}18)$$

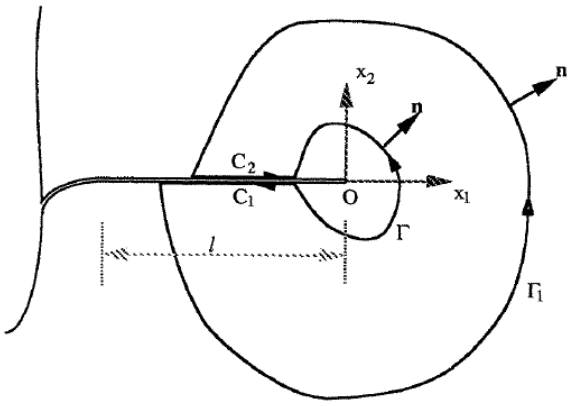

Figure 4.7. The line contour for j. Γ is shrinking onto 0 by definition (not shown in the plot) (Rice et al. 1968)

These calculations of J-integral can still be related to SIF by $J = G = \frac{K_I^2}{E}$.

Feng et al. also provided the analytical solution of the SIF for an unbridged and bridged fracture generated at the wellbore surface undergoing in-situ stresses and wellbore pressure using the geometry below (Feng, 2016 (a)). The SIF is calculated by using Equation 4-19 and the geometry illustrated in Figure 4.8. S_{hmax}, S_{hmin} are interchangeable with σ_H, σ_h , representing the maximum and minimum horizontal stress, respectively

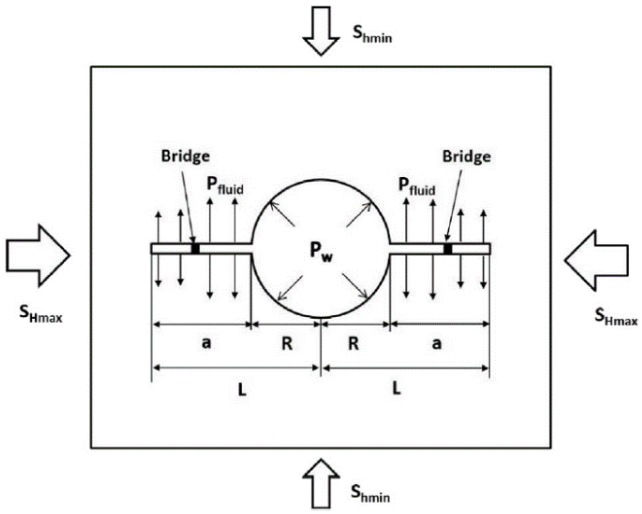

Figure 4.8. Geometry used to calculate stress intensity factor (Feng et al. 2016 (a))

$$K_I = (F_1 + F_2) * [2 * p_w - (S_{hmax} + S_{hmin})] + (F_1 + 3 * F_2) * (S_{hmax} - S_{hmin}) - 2 * F_4 * (p_w - p_p) \quad (4\text{-}19)$$

$$F_1 = \frac{1}{\sqrt{\pi a}} \int_R^L G(r)dr$$

$$F_2 = \frac{1}{\sqrt{\pi a}} \int_R^L \frac{R^2}{r^4} G(r)dr$$

$$F_3 = \frac{1}{\sqrt{\pi a}} \int_R^L \frac{R^4}{r^4} G(r)dr$$

$$F_4 = \frac{1}{\sqrt{\pi a}} \int_D^L G(r)dr$$

$$G(r) = \frac{1.3 - 0.3 * \left(\frac{r - R}{a}\right)^{\frac{5}{4}}}{\sqrt{1 - \left(\frac{r - R}{a}\right)^2}}$$

where p_w and p_p are wellbore pressure and pore pressure behind the fracture, respectively. D is the radial distance from the bridge location to the wellbore center. When there is no bridge in the fracture, D and F_4 will all become zero.

4.3 Fundamental equations for multi-physic coupling of thermoporoelasticity processes.

Thermal stress induced during lost circulation is controlled by three primary processes: temperature change of the formation, redistribution of pore pressure as fluid invades, and thermal stress generated within the rock matrix. Pore fluid flow within the formation leads to a redistribution of the formation's temperature due to its convective and conductive effects. Poroelasticity with a combined mechanical and hydraulic processes during lost circulation accounts for the pore pressure and stress variation near the wellbore region. Thermal expansion of the solid/fluid system connects temperature redistribution with poroelasticity and generated thermal stress.

The three mechanisms are combined in this finite element (FE) analysis. In this study, the following fundamental equation is adopted to govern the heat transfer process within the formation matrix (COMSOL, CFD Module User Guide):

$$\left(\rho C_p\right)_{eq} \frac{\partial T}{\partial t} + \rho C_p \mathbf{u} \cdot \nabla T = \nabla \cdot \left(k_{eq} \nabla T\right) + Q \tag{4-20}$$

This equation is a general description of the heat transfer process in porous media. Both heat conduction and convection caused by the invasion of mud into the formation are considered in this system. $\left(\rho C_p\right)_{eq}$ and k_{eq} in Equation 4-20. represents the equivalent volumetric heat capacity and the equivalent thermal conductivity of the fluid-solid system, respectively. They are calculated in FE process using the thermal conductivity and thermal capacity of both the rock matrix material and porous fluid. The rock matrix is considered to be fully saturated and that both the invasion

fluid (mud) and original fluid (reservoir fluid) properties are equal. Thus both $\left(\rho C_p\right)_{eq}$ and k_{eq} mentioned above can be obtained by using the porosity of the formation. **u** refers to the velocity field of pore fluid, which controls the heat convection caused by fluid leak-off (invasion of mud) through wellbore and fracture boundaries. This FE simulation uses Darcy's flow as the main mechanism to determine the velocity field. This can be expressed in the following format:

$$\mathbf{q} = -\frac{k}{\mu}\nabla p \tag{4-21}$$

The local pore pressure distribution (hydraulic part of the model) and stress fields (mechanical part of the model) are also combined in the model using the following thermo-poroelasticity principles (4-22) - (4-24) (Holzbecher, 2013).

$$s - s_o = C \cdot (\varepsilon - \varepsilon_o - \varepsilon_T) - \alpha p \tag{4-22}$$

$$\varepsilon_T = \alpha_T \left(T - T_{ref}\right) \tag{4-23}$$

$$\rho_f S \frac{\partial p_f}{\partial t} + \nabla \cdot (\rho \mathbf{q}) = Q_f - \rho_f \alpha \frac{\partial \varepsilon_v}{\partial t} \tag{4-24}$$

The definition of this stress-strain relationship mentioned above considers both the thermally induced strain and pore pressure, as shown in Equation (4-22). Thermal stress is incorporated into the modeling by induced thermal strain, denoted by ε_T, of rock matrix, as shown in Equation (4-23). Pore pressure in this study is found by coupling the velocity field **q** from Darcy's law with the following continuity equation (COMSOL, Subsurface Flow User Guide).

$$\frac{\partial}{\partial t}(\rho\phi) + \nabla \cdot (\rho \mathbf{q}) = Q_m \tag{4-25}$$

ϕ is defined as the porosity of the porous media. Q_m is the mass going in or out of the pore space. By considering density and porosity, both as functions of pressure, $\frac{\partial}{\partial t}(\rho\phi)$ can be transformed into $\rho_f S \frac{\partial p_f}{\partial t}$. S is a storage coefficient with the unit 1/Pa and can be interpreted as the weighted compressibility of bulk materials and fluid within the pore space. At the same time, we need to consider the change of porous space volume when we calculate the flow of pore fluid.

Therefore Q_m can be expanded to $Q_f - \rho_f \alpha \frac{\partial \varepsilon_v}{\partial t}$ to involve the deformation of the rock matrix with ε_v to denote the volumetric strain of the solid phase in a porous media. Thus, the continuity equation transforms into the following generalized equation that gives us the pore pressure distribution:

$$\rho_f S \frac{\partial p_f}{\partial t} + \nabla \cdot (\rho \mathbf{q}) = Q_f - \rho_f \alpha \frac{\partial \varepsilon_v}{\partial t} \quad (4\text{-}26)$$

Biot's coefficient α appears in this part of the equation as a weighting factor for the impact of pore pressure. It is also included in Equation (4-24) to compute the pore pressure. Pore pressure in this model affects the stress-strain variation and deformation of the porous media. Meanwhile, the change of the stress/strain state in porous media will also influence the pore pressure distribution conversely, as implied in the poroelasticity Equation (4-26). In the transient FE study utilized this study, the effects of hydraulic and mechanical modeling need to be taken in to account simultaneously.

Chapter 5. Methodology

5.1 General description of finite element method

Due to the inherent complexity of lost circulation problems, we choose the finite element method (FEM) as our tool to study the stress state of a fractured wellbore. Unlike analytical solution that seeks the exact answers, FEM is one of the numerical methods that seeks for approximate solutions of mathematical problems. The laws of physics for space- or time-dependent problems are usually described in a partial differential equation. Analytically solutions of these equations can be extremely difficult to achieve, sometimes impossible, when real-life problems are encountered. Instead, an approximation of the initial solution can be constructed. A simple explanation of FEM is to represent real objectives by a simplified geometry, discrete it into elements, describe the behavior of each element individually, and reconnect these elements at nodes, which is called meshing in finite element [Salehi, 2012]. The meshed geometry of a fractured wellbore is showed as an example in Figure 5.1. In-situ stresses, initial temperature, and pore pressure distribution, are pre-set on the domain of formation rock as initial conditions. Pressure, fluid invasion rate, and temperature are presumed as boundary conditions on wellbore and fracture surface. Stress field, displacement of the whole geometry can be deducted from outer boundary to inner nodes and elements according to the basic law of physics predefined within the objective model.

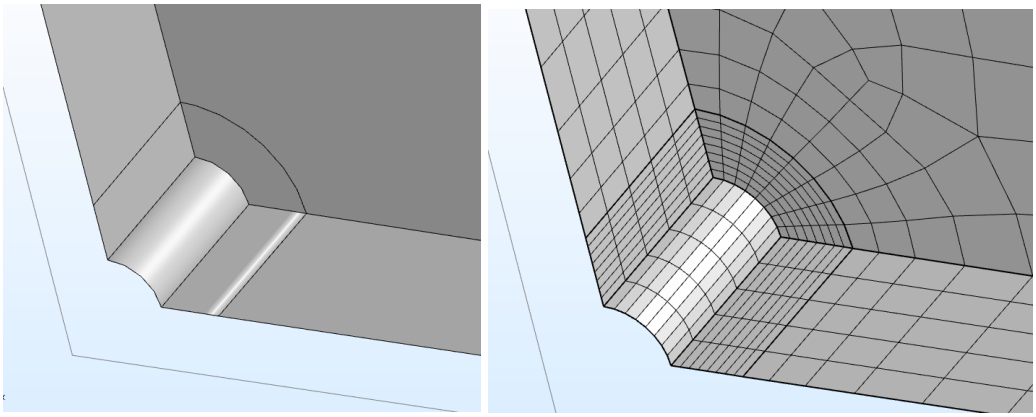

Figure 5.1. Meshing a geometry in finite element software: the example of a fractured wellbore.

FEM has obvious advantages over analytical solutions when it comes to the analysis of objectives with irregular geometries and complicated physic conditions. FEM software offers high flexibility to build models with a variety of shapes. The Stress state in the near wellbore region during lost circulation is influenced by a combined effect of initial stress state, the hydraulic pressure in the wellbore, and fluid invasion into formations. When temperature change and thermal effect comes into play, this problem becomes even more complicated. Coupling of the multi-physics process including stress change, heat transfer, and fluid flow is difficult in a mathematical meaning. The primary task for a multi-physic study is to identify governing equations from each physics and apply them appropriately to specific situations. The next and the most formidable task is to solve these processes simultaneously with each physic well coupled with others. FEM is considered an efficient and relatively accurate method to solve a multi-physic problem.

5.2 Finite element modeling of a fractured wellbore with thermoporoelasticity

The three-dimensional model used in this thesis for the finite element method was designed to represent a section of a vertical wellbore with two short fractures generated asymmetrically from the wellbore. For this study, a 3D model was preferred over a 2D model because of the capability of the FE software. The 3D simulation presents a more robust and stable result compared to the

2D model when coupling the heat transfer and poroelasticity processes. Figure. 5.2(a). Illustrates the cross-sectional area of the entire fractured wellbore's geometry. To consider pre-existing fractures in lost circulation and WBS, two narrow eclipse-shaped voids were established on the wall symmetrically in the x-direction. The length of the model is much larger than the wellbore diameter and fracture length so that the boundary effect on the stress around the wellbore and fracture is negligible. In situ minimum and maximum horizontal stresses, S_{hmin} and S_{hmax} were applied to the whole domain of the model as the initial stress state. The same wellbore pressures were implemented on both the inner wall of the wellbore and fracture surface. Owing to the asymmetrical feature of this problem in the horizontal direction (X-Y Plane), only a quarter of the entire geometry is needed in the finite element study. Two symmetrical boundaries extending in the Z direction are then established, as is displayed in Figure. 5.2(b). Uniformed pressure boundaries were set up along wellbore wall and fracture surface. This study utilizes four nodes quadrilateral meshes on an upper plane that sit on an x-y plane and sweep the geometry along z direction to generate 8-nodes hexahedral elements for the 3D model, as showed in Figure 5.2(b).

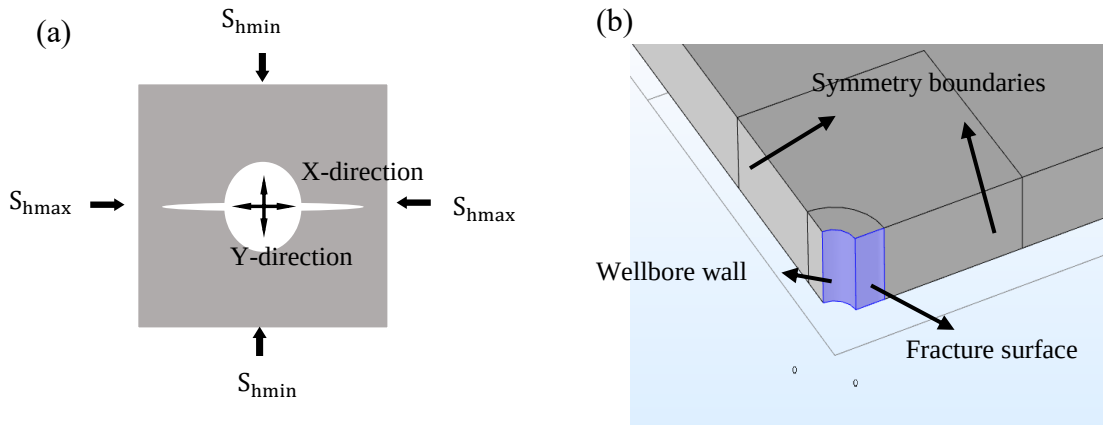

Figure 5.2. Simplified diagram of (a) the cross-section of the whole wellbore and (b) 3D geometry established in the finite element study (a quarter of the entire model with asymmetrical boundaries).

When the drilling fluid gets in contact with the formation, the formation's temperature will gradually decrease owing to the wide difference in the temperature of the drilling fluid and the formation. The presented simulation accounts for fluid leakage into the formation assuming that a mud cake does not form to restrict fluid flow. The reservoir temperature is applied to the model's domain as an initial condition, while the wellbore fluid temperature is being implemented to the inner boundary. The simulation couples fluid flow with a thermal interaction between the drilling fluid and porous matrix. This study combines thermal stress with both linear elasticity and poroelasticity models by integrating thermal expansion into the simulation. This combination can successfully demonstrate the impact that a drop in temperature has on the formation when redistributing the stress.

The concept of hoop stress is utilized in this study to analyze the stress along the wellbore and fracture surface. The hoop stress denotes the circumferential stress or tangential stress at 90° to the radial direction from the center of this system as a component of a cylindrical coordinate system. The hoop stress along the wellbore is the tangential stress that indicates the magnitude of compression or tension experienced by the wellbore wall (Feng et al. 2016a, Feng et al. 2016b, Tada et al., 1985). Along the fracture surface, the hoop stress is the stress perpendicular to the direction of the fracture acting to close the fracture. This study denotes compressive stress as positive and tensile stress as negative. The hoop stress can be interpreted as the compressive state of formation; thus, it can be used as an indicator of fracture re-initiation or propagation. As the hoop stress decreases, the likelihood of the fracture to be reinitiated increases.

5.3 Boundary conditions and input data

This section specifies boundary conditions and input data adopted to develop the 3D finite element model. The model's geometry and physical input data are established based on the data used by Feng in his 2016 paper with some adjustments (Feng et al. 2016b). The original 3D wellbore geometry of the model is comprised of a 160-inch long block with a 4.25-inch radius circle subtracted from the center of the square. A bi-wing eclipse-shaped fracture with 6-inch half-lengths emanates symmetrically from the wellbore wall in the x-direction. In situ stress consists of maximum horizontal stress S_{hmax} = 3,600 psi along the fracture direction, and a minimum horizontal stress S_{hmin} = 3000 psi perpendicular to the fracture direction. The initial formation pore pressure was set at 1,800 psi.

5.3.1 Boundary conditions set up for lost circulation scenarios

In lost circulation scenarios with no fluid restrictions in the fracture, a 4,000psi wellbore fluid pressure (p_{wf}) was applied to the wellbore surface boundary and along the fracture surface to support its opening and provide overbalanced fluid pressure. The fluid flow was controlled by specifying the inlet flow velocity through the wellbore and fracture surface.

The thermal conditions for different initial states and boundary conditions of this model, which drives the redistribution of wellbore stress, will be specified in this subsection. The formation's initial temperature was set at 180°F, and a variety of fluid temperatures were applied to the wellbore and fracture surface to compare the changing stress redistribution. The transmission of heat between the relatively cold wellbore fluid and the warm formation was coupled with the fluid leakage mentioned above. The necessary parameters that are known to affect the thermal stress are listed in Table 5.1., together with other input data used in this model. This data was compiled from previous research about WBS and wellbore temperature discussion (Feng et al. 2016b, Kabir et al.

1996). Mechanical related data like Young's modulus and in situ stress and so on in Feng's paper are manipulated according to standard ranges of these parameters of formation in certain depth. Thermal properties of drilling-related materials are from tests in the field according to Kabir's work (Kabir et al. 1996).

Table 5-1. Model input data

Parameters	Symbol	Value
Model length	L	160[in]
Wellbore radius	R_w	4.5[in]
Young's modulus	E	1,000,000[psi]
Poison's ratio	ν	0.2
Minimum horizontal stress	S_{hmin}	3,000[psi]
Maximum horizontal stress	S_{hmax}	3,600[psi]
Initial pore pressure	p_{pore}	1,800[psi]
Wellbore pressure	p_{wf}	4,000[psi]
Fracture length	L_f	6[in]
Fluid leak-off rate	v_{in}	1[in/min]
Rock Permeability	K	100[mD]
Rock Porosity	Φ	0.3
Rock density	ρ_r	22[lbm/gal]
Rock thermal conductivity	K_r	0.87[Btu ft/ h/ ft^2/°F]
Rock thermal expansion coefficient	α_T	3E-4[1/°F]

(table cont'd.)

Parameters	Symbol	Value
Rock specific heat (Heat capacity)	C_r	0.19[Btu /lbm/°F]
Drilling fluid density	ρ_r	12[lbm/gal]
Initial reservoir temperature	T_r	180°F
Wellbore fluid temperature	T_{wf}	120°F

5.3.2 Boundary conditions set-up for WBS implementation: fracture plugging and the inner filter cake

Implementation and effectiveness of WBS are closely associated with wellbore cooling effect and induced thermal stress. A temperature drop of formation due to cold mud invasion leads to the thermal contraction of formation rock and pore pressure redistribution, all contributing to the stress state in near wellbore area. Short fractures generated on the wellbore as a result of overbalance drilling provide a much more convenient channel for fluid leak-off into the formation. This intensifies the cooling process of formation and dramatically increased the magnitude of thermal stress. WBS operations prevent fracture propagation through bridging and plugging fractures and elevate hoop stress state around wellbore wall. This also intercepts the processes of fluid invasion and heat transfer. Thermal effect on fracture stability and the risk of fracture re-initiation when WBS is applied could differ from the simply lost circulation scenario. This study takes a step further to study the thermal effect on fractures to evaluate whether WBS effectiveness would be affected or weakened when a large temperature difference exists between reservoir to be drilled and the wellbore fluid.

Though those three mechanisms of WBS mentioned above might take effect simultaneously in practice, they are studied separately in this study to clarify their individual effect. Stress cage theory is not examined in this study for several reasons. Stress cage explanation of WBS involves

hoop stress enhancement of near-wellbore area as a whole, the result on fracture tip or fracture propagation resistance is barely discussed. Other factors related to cooling process and thermal stress such as pore pressure and fluid leak-off are also not out of considerations. Stress change around wellbore under stress cage theory can be studied together with closure pressure.

Extending previous finite element simulations for lost circulation, this thesis implements WBS in two scenarios: 1) fracture bridging/plugging to test thermal effect under fracture tip isolation and fluid restriction in the wellbore; 2) Inner filter cake buildup on fracture surface to test the thermal effect with permeability redistribution in near-wellbore area.

In WBS implementation through fracture bridging/plugging, the fracture is plugged with lost circulation materials (LCMs) as shown below in Figure 5.3. In this work, the plug formed inside the fracture by LCMs across the fracture width is called an LCM bridge. For the simplification of the model, it is assumed that LCM would form a "perfect" bridge that represents a rigid body with zero permeability, which allows no fluid flows across the bridge. The essential function of LCM bridge is a fluid restriction or fracture tip isolation. Drilling fluid invasion into fracture will be restricted or prevented by the LCM bridge. And with the permeability of formation rock, fluid inside fracture between the LCM bridge and fracture tip will still dissipate naturally into surrounding formations. Fluid pressure and temperature in this part of fracture space behind the bridge are thus released and maintained at the same pore pressure as in the porous media that neighboring fracture tip. Such effect is created by setting zero fluid leak-off rate along the fracture surface behind the LCM bridge. Fluid pressure acting on fracture surface will be specified as the same with surround pore pressure. While wellbore pressure, fluid leak-off and wellbore fluid temperature remain consistent on the fracture surface in front of the bridge, convective heat transfer strengthened by fluid loss is thus restricted within this region. The LCM bridge protects

fracture tip from the direct contact with high wellbore pressure and low wellbore temperature. However, temperature variation could still play an important role in the stress change in near wellbore area. By setting up the LCM bridge in the fractured wellbore model, the author would be able to evaluate how temperature effect could possibly undermine the WBS implementation by bridging and plugging the fractures, especially when the fracture is plugged in varies positions.

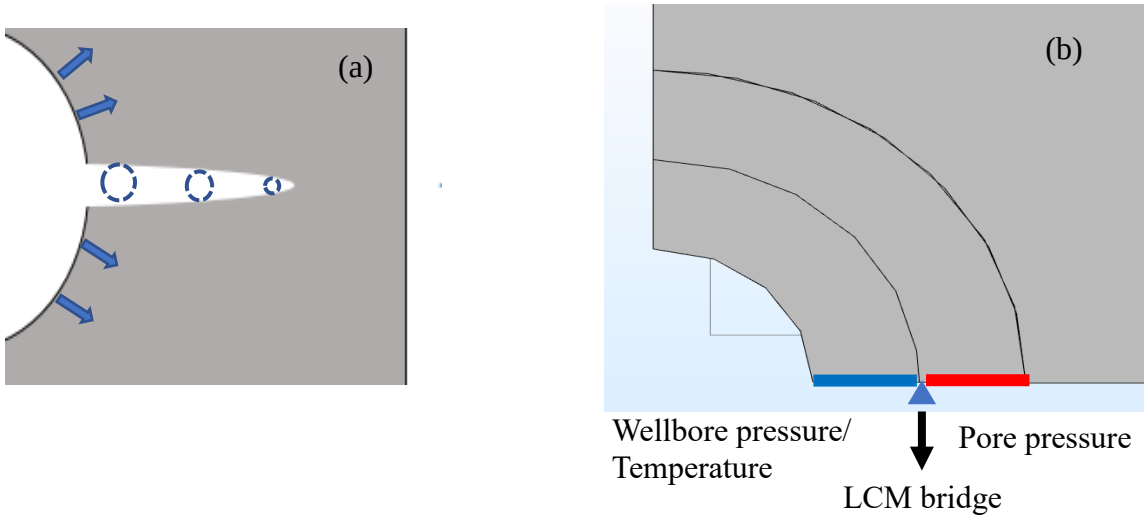

Figure 5.3. a) WBS strengthening with different plugging positions b) Boundary loading conditions at fracture surface when LCM plug is applied.

WBS implementation through FPR assumes finer materials would first infiltrate into the formation through fracture surface and create a thin layer of the zone with sufficient low permeability. Since this hypothesis allows pressure communication from the wellbore to fracture tip, it is necessary to adjust the boundary set-up to evaluate the fluid restriction and formation cooling effect considering different inner filter cake permeability. Previous sections regarding fracture plugging control the fluid leak-off through one section of fracture surface to be consistent and uniform throughout the simulation, when this section contains the same wellbore pressure boundary. As long as formation properties remain unchanged, fluid leak-off into the formation is

only related to wellbore fluid pressure. However, with internal filter cake build-up, fluid leak-off would vary, even with the same wellbore pressure. Therefore, the simulation to evaluate the effect of internal filter cake by using constant inlet pressure rather than constant leak off rate to control fluid flow. Pressure and temperature boundaries in this section of the simulation are illustrated in Figure 5.4a). Internal filter cake is fulfilled in the FE modeling with a thin 1mm thick layer that covers fracture surface and fracture tip, as showed in Figure 5.4b).

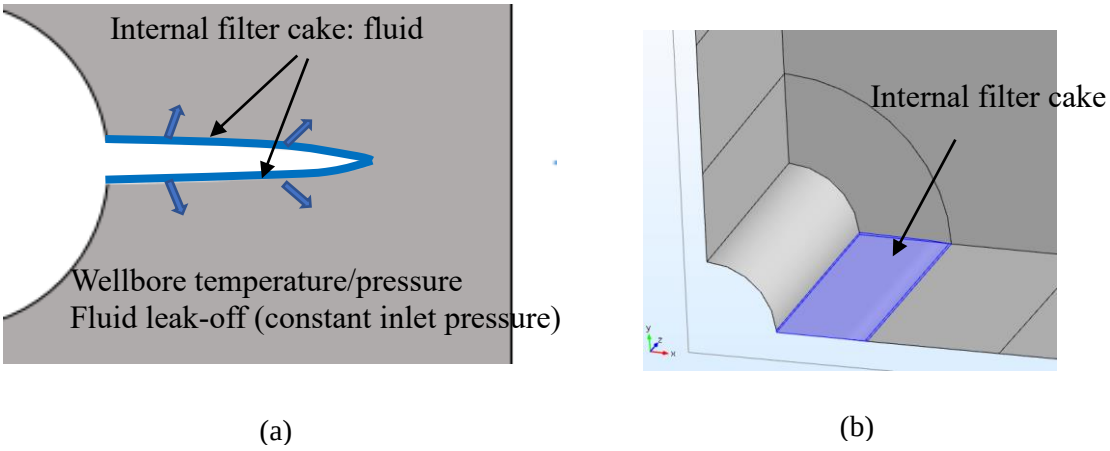

Figure 5.4. a) Boundary loading conditions for WBS implementation through internal filter cake build up and b) Internal filter cake build up inside the fracture surface, represented by a thin layer of material with different permeability.

Chapter 6. Preliminary Model Verification

6.1 Unbridged fracture: SIF at fracture tip under isothermal condition

One of the primary objectives of this study is to investigate the effects of induced thermal stress on the fractures generated during lost circulation. Hoop stresses along the fracture surface, in this case, could be an excellent reference to test the possibility of fracture re-initiation and propagation. Unlike the breakdown pressure of an intact wellbore, the stress state at the fracture tip cannot be translated directly into the fracturing pressure. Thus, general criteria for fracture initiation at the fracture tip need to be utilized to evaluate the stress state at the fracture tip. However, analytical solutions that express the stress state at the fracture tip are rare. Several analytical solutions for the stress intensity factor at the fracture tip with two small pre-existing fractures symmetrically emanating from an elastic wellbore have been proposed in the past. The detailed calculation can be found in the theoretical background of this thesis.

For the unbridged fracture in this study, the SIF can serve as a useful parameter to verify the accuracy of the presented finite element study. In this thesis, SIF was first obtained from the finite element analysis using increasing maximum horizontal stress, under isothermal condition. The results are validated by the comparison with an analytical solution with pure linear elasticity, also under isothermal condition. To stay consistent with the assumptions in analytical solution, no fluid invasion will be set up through the wellbore and fracture surface. Detailed calculation methods used in the finite element study can be found in Chapter 4. The results were compared with SIFs obtained from the analytical solution (Feng et al., 2015). The minimum horizontal stress, S_{hmin}, was set to 3000 psi; the maximum horizontal stress, S_{hmax}, increase from $1*S_{hmin}$ to $2*S_{hmin}$; and the wellbore pressure p_{wf} was set to 4000 psi. The comparison showed in Figure 6.1. partially

demonstrates the validity of the finite element study presented in this work because of how close they match.

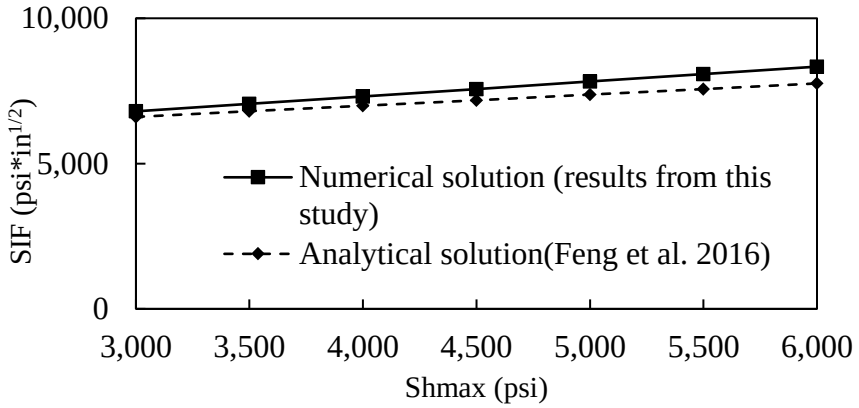

Figure 6.1. Comparison of the SIF obtained in this study and that obtained from the analytical solution. Fluid leak-off is not considered.

6.2 Unbridged fracture: Induced thermal stress at fracture tip

Simulation results of this thesis can also be partially validated by hoop stress change at fracture tip due to thermal effect. Although the SIF has been defined to measure the stress at the fracture tip, compelling solutions for the stress state at the fracture tip under a thermal effect are rare. However, changes in the hoop stress due to the thermal effect along an intact wellbore has long been proposed analytically and adopted as the variation in fracture pressure, as shown in Equation (6-1), based on the thermoelasticity theory (Fjær et al., 2008).

$$\Delta\sigma_\theta = \frac{E}{1-\nu}\alpha_T(T_r - T_{wf}) \tag{6-1}$$

$\Delta\sigma_\theta$ is the hoop stress variation along wellbore due to temperature change; E and ν are Young's modulus and Poisson's ratio, respectively; α_T is the thermal compressibility, and $(T_{wf} - Tr)$ represents the difference in temperature between the drilling mud contained in the wellbore and the initial reservoir temperature. Figure 6.2. shows the induced thermal stress on an intact wellbore.

Its agreement with analytical solution also provided a partial verification of induced thermal stresses calculated from the numerical soliton in this work.

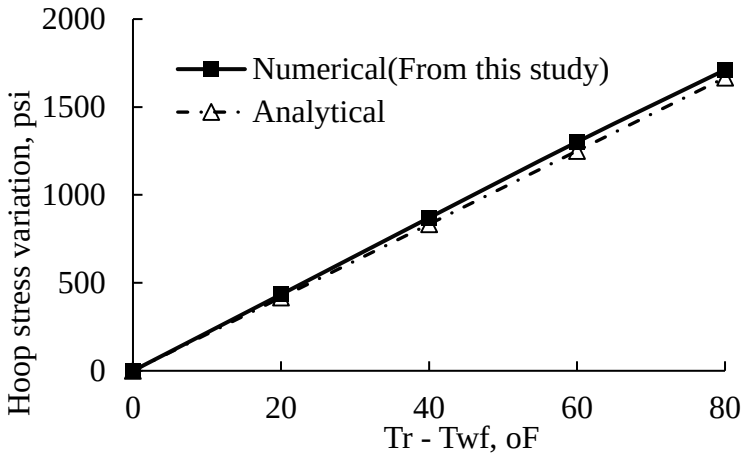

Figure 6.2. Comparison between hoop stress change on intact wellbore obtained in this study and the fracture gradient change under the cooling effect obtained from the analytical solution

6.3 Fracture with perfect bridge: WBS implementation at different positions

The difference in fracture plugging position could considerably influence the temperature and loading conditions on fracture surface, as shown in Figure 6.3. below. When the fracture is completely plugged at fracture mouth, the fracture contains only pore pressure and the temperature remains the same with surrounding formations. Fracture tip, in this case, is well isolated from lower temperature and high wellbore pressure in the wellbore. As the plugging position moves closer to fracture tip, fracture starts to undertake higher tensile stress stemming from the wellbore pressure/temperature inside fracture space that leads to the possible fracture propagation.

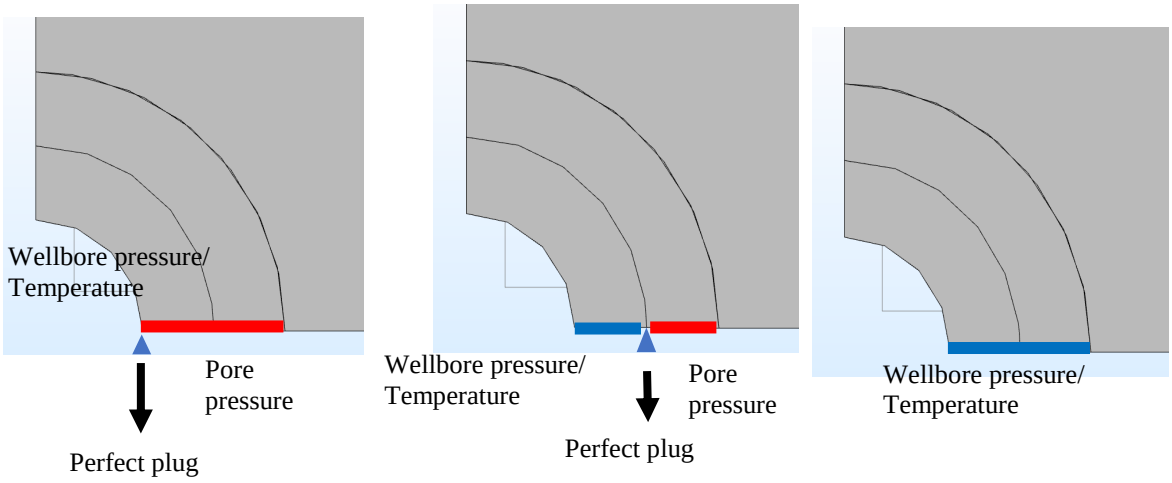

Figure 6.3. Boundary loading conditions at fracture surface when LCM plug is applied at different locations: a) the fracture is fully plugged at fracture mouth b) fracture is plugged at the middle of fracture; c) fracture is plugged at fracture tip (no plug). Pressure and temperature boundary are maintained on wellbore wall throughout the simulation.

In this section, WBS is first implemented in pure linear elasticity and thermoelasticity without considering poroelasticity and pore pressure in the formation. Analytical solutions for SIF under different plugging position are available from several previous types of research with a linear elastic fracture initiation criterion. A typical one is derived by combining Kirsch stress solution around a circular borehole (Feng et al., 2016). His model calculates SIF by taking into consideration wellbore and fracture geometry, load conditions, and fracture plugging. Feng's calculation of SIF is based on the geometry below with a circular wellbore and two short fractures symmetrically located at both sides of the wellbore. His model also adopted pore pressure in the fracture zone that is isolated by LCM bridge, same loading conditions used in this work. Regretfully these analytical solutions all assumed an isothermal condition.

FE modeling of SIF proposed in this thesis can be partially validated against the analytical solutions from previous papers by comparing results when pure linear elasticity is adopted in the simulation. As shown in Figure 6.4., plugging position can significantly influence the SIF at

fracture tip. When the perfect plug is set-up near fracture tip, SIF is still rather high, meaning a strong tendency of fracture initiation. As LCM bridge build up closer to fracture mouth, SIF gradually decreases from positive to negative, showing that the stress state at fracture tip is changing from tensile stress to compressive stress. The decreasing SIF as the fracture is plugged by LCM bridge clearly presents that bridging the fracture reduces the risk of fracture initiation. When SIF is lower than KIC, the critical SIF for fracture initiation, the fracture will no longer be able to propagate under current conditions. The good accordance between the results from numerical simulation in this thesis and analytical solution under linear elasticity validated the effectiveness of this model.

Formation cooling effect, according to Fig. 6.4., increases SIF and strengthen the tendency of fracture initiation. In isothermal condition, the SIF's decline with plugging position close to fracture mouth showed an approximately linear relationship. SIF's change under cooling effect, however, showed less linearity. SIF maintains a relative flattened change when LCM bridge plugs in the middle of the fracture. This leads to a gradually enlarged SIF difference between an isothermal condition and cooling condition as the bridge moves away from fracture tip. While fracture tip under isothermal condition reaches to compressive stress state Such tendency means the influence of formation cooling is relatively stronger when the plugging happens around at the middle position of fractures. As the fracture becoming filled up by LCM completely when the fracture is plugged near the mouth, SIF under cooling effect starts to drop in a steeper slope and the cooling effect become less important. This also conform with our experiences that when fracture tip is isolated from wellbore temperature, the influence of cooling effect is reduced to a minimum.

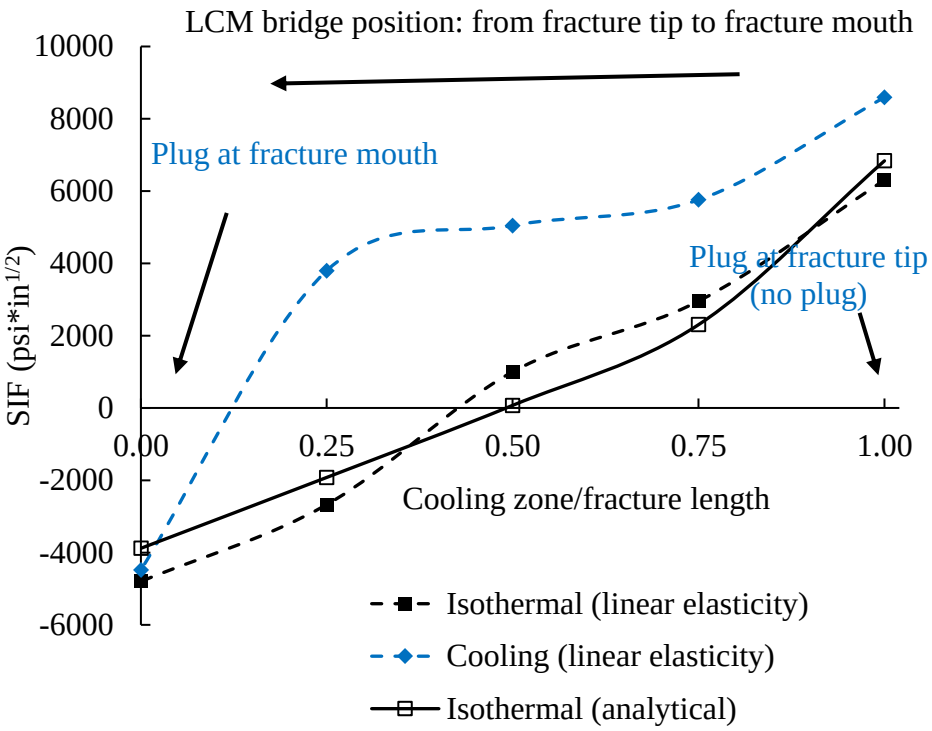

Figure 6.4. SIF at fracture tip when LCM plugs are applied at different positions in fractures, with and without considering wellbore cooling effect. No poroelasticity considered.

Chapter 7. Results and Discussions

7.1 Thermal stress induced along wellbore wall during lost circulation with unbridged fractures

7.1.1 Comparison between thermoelasticity and thermoporoelasticity (with and without pore pressure)

Stress redistribution as the formation cools was first analyzed in a thermoelasticity model without any consideration of pore pressure. The establishment of the linear elasticity model provides a demonstration of how the stress state changes along the fracture. The hoop stress along the wellbore and fracture surface were obtained using a cylindrical coordinate system. The results were then compared with the thermo-poroelasticity simulation. As the high-temperature reservoir (180°F) interacts with relatively cold mud (120°F) at the wellbore and fracture surface, heat transmission in these two cases occurs only in the form of conductive heat transfer. To better plot the results, the hoop stress along wellbore wall is plotted by the clockwise rotation angle to the maximum horizontal stress. The range is from 0° to 90°, taking the angle at the fracture mouth to be 0°. The hoop stress along the fracture surface is plotted along the distance away from the wellbore wall. These two types of plotting were also adopted in the following section. Hoop stress was first generated without considering any thermal effects (refer to “isothermal condition” in the following figures). The result was then compared with the hoop stress while the formation was cooled by using a lower temperature along the wellbore and fracture face (refer to “cooling” in the following figures).

The previous section is applicable only when drilling is done into a formation with very low permeability, such as shale. However, when a lost circulation process is the emphasis of the model, the fluid leakage rate will become the dominant parameter controlling the heat exchange and thermal stress. Therefore, a poroelasticity model is adopted in this section to present more

representative results. The initial reservoir pore pressure p_{pore} was set at 1800 psi, and a relatively small leak-off velocity v_{in} = 0.1 inches/minute was predefined at the wellbore formation interface in the poroelasticity domain. The initial reservoir and wellbore temperature, in this case, are 180°F and 120°F, respectively.

In both the thermoelasticity model with no pore pressure and thermo-poroelasticity model, the hoop stress decreases dramatically along the wellbore when the wellbore is cooled down, especially at 90° to the maximum stress direction (Figure 7.1.). It could be observed that the hoop stress reduction due to wellbore cooling remains constant. The hoop stress, however, in the poroelasticity model was seen to be lower than that in the linear elasticity model due to pore pressure.

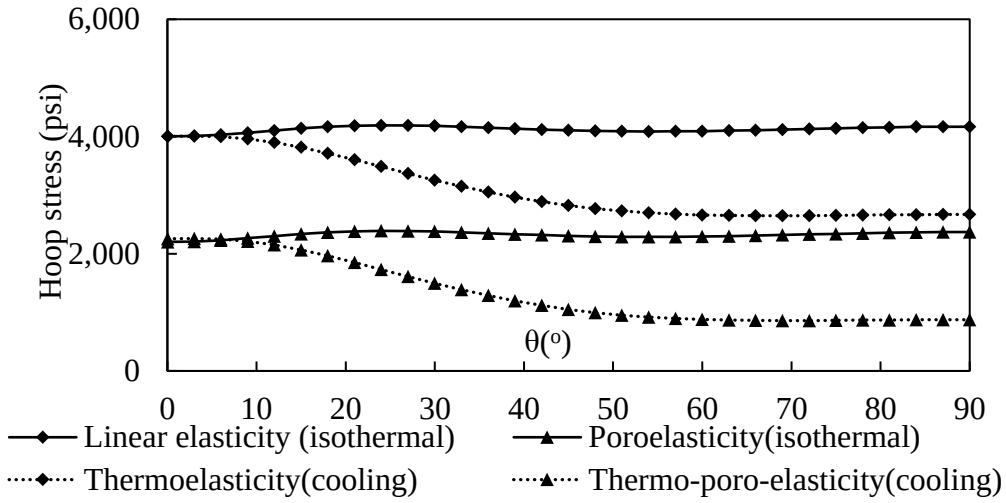

Figure 7.1. Thermal impact on hoop stress along the wellbore wall.

Figure 7.2. shows that the hoop stress along the fracture face is also reduced considerably near the tip when considering the effects of cooling. This variation in stress indicates decreasing compressive stress during the cooling process of the formation rock. Such a phenomenon reveals

that the tensile stress is more likely to occur in the fractured area, which will increase the chance of reinitiating the fracture.

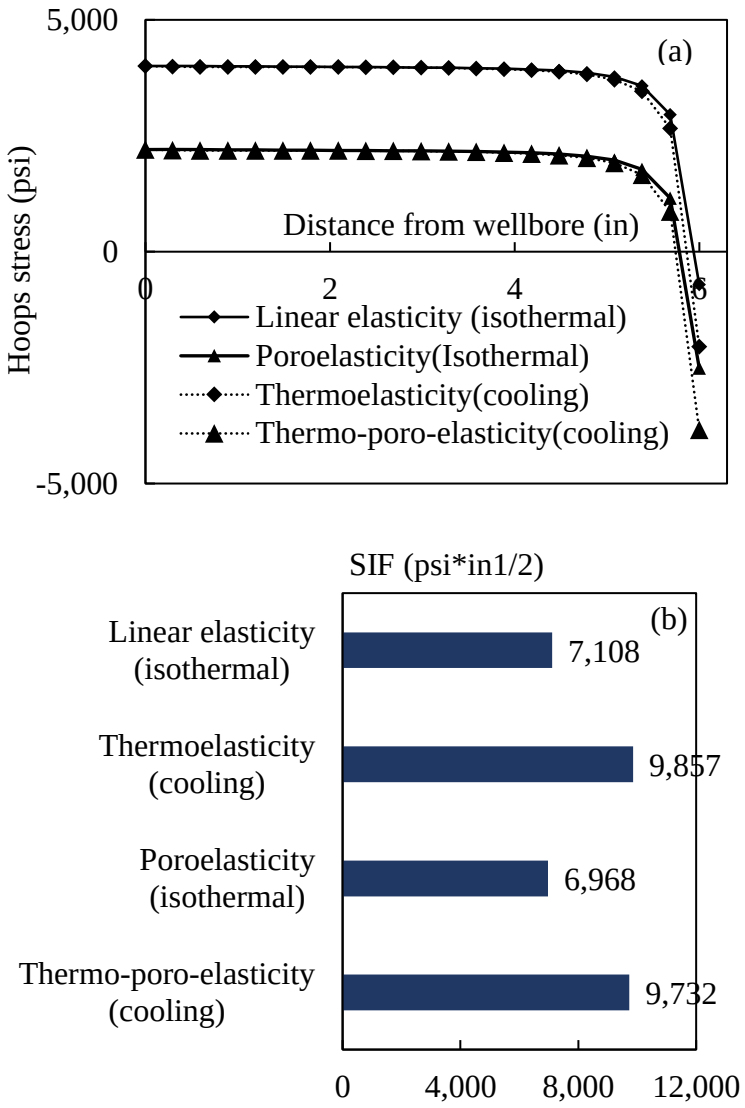

Figure 7.2. a) Thermal impact on hoop stress along the fracture surface and b) SIF at fracture tip. Both the linear elasticity model and poroelasticity model with constant pore pressure were considered.

Here, the SIF for both cases was collected and compared to analyze the effect of thermal stress on the initiation of pre-existing fractures. The simulation results showed both the elasticity model and poroelasticity model with pore pressure had similar SIF increases, indicating the variation in

pore pressure. Cooling the formation did not have a significant effect on the initiation of the fracture under the thermal effect even though it does have an impact on the stress state around the fracture tip. Additional interpretations of the role of the pore pressure during wellbore cooling are provided in the sections that follow.

7.1.2 Parametric Study on Wellbore Temperature

One of the major forces that drive the redistribution of near wellbore thermal stress is the temperature difference between the wellbore fluid and the formation. In this section, a sensitivity analysis of the stress redistribution of the formation with different wellbore fluid temperatures was compiled. The initial fluid temperatures were 80°F, 115°F, and 150°F, while the initial reservoir temperature was set at 180°F. The initial pore pressure of the reservoir $p_{pore}$was set at 1800 psi.

As shown in Figure 7.3a), the difference between the initial temperature of the reservoir and the drilling fluid has a significant impact on the final hoop stress. This phenomenon suggests that an enormous risk of re-initiating the fracture once the high-temperature reservoir is in contact with the drilling fluid exists. Such an occurrence would undoubtedly jeopardize the wellbore's stability. Conversely, ignoring the thermal effects during the drilling design process will lead to an overestimation of wellbore stability. The maximum decrease in the hoop stress on the wellbore wall caused by thermal shock can also be observed in Fig. 6b.The results show an excellent agreement with the analytical solution obtained from Equation $\Delta\sigma_\theta = \frac{E}{1-\nu}\alpha_T(T_{wf} - T_r)$, as is illustrated in Figure 7.3b). Unlike an intact wellbore, a wellbore with existing fractures does not undergo uniform stress reduction owing to the temperature change. The maximum hoop stress variation occurs at the wellbore along the same direction as S_{hmax}, as is shown in Figure 7.3b)., while the hoop stress at the fracture mouth would remain almost the same. These results imply that, in such a situation, when the fracture has already been generated, it is very likely for the

wellbore failure to occur in the same direction as the minimum horizontal stress direction when a large temperature difference exists.

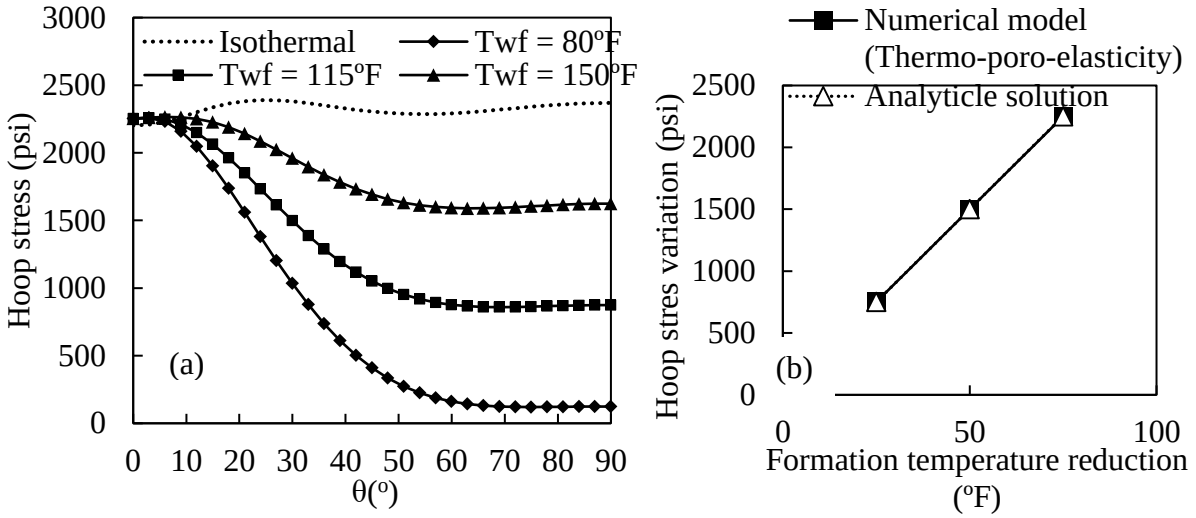

Fig. 7.3. (a) Hoop stress variation along the wellbore wall under the thermal effect. (b) Maximum stress change (90º to the fracture mouth) are compared with the analytical model.

The results plotted in Figure 7.4. show that, under the thermal effect, the hoop stress does not change along the fracture face, but it drops at the fracture tip. The change in hoop stress indicates that the fracture tip is subjected to a higher tensile stress when the formation confronts the lower temperature drilling fluid. The SIF at the fracture tip confirmed this observation.

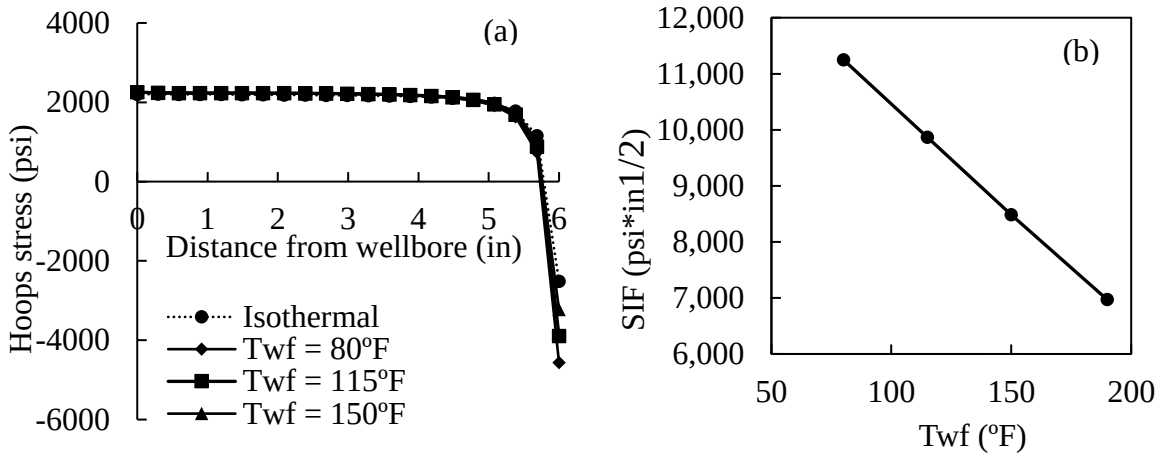

Figure 7.4. (a) Hoop stress along the fracture face and (b) SIF under the formation cooling effect.

7.1.3 Parametric Study on Maximum Horizontal Stress

In this study, simulations of different maximum horizontal stresses were conducted while maintaining the same minimum horizontal stress. The minimum horizontal stress S_{hmin} was set at 3000 psi with increasing maximum horizontal stresses S_{hmax}/S_{hmin}= 1, 1.3, 1.6 and 2. Figure 7.5. below shows that an increase in the hoop stress occurs when the maximum horizontal stress increases. When a strong anisotropy exists in the formation, strong compressive stress will occur in the wellbore at 90° to the maximum horizontal stress. Such an increase indicates growing compressive stress, and relatively high wellbore stability of the wellbore when there is high maximum horizontal stress. The results in Figure 7.5. show that, for the same pore pressure state, stress reduction due to the formation cooling process remains the same for different horizontal stress constants.

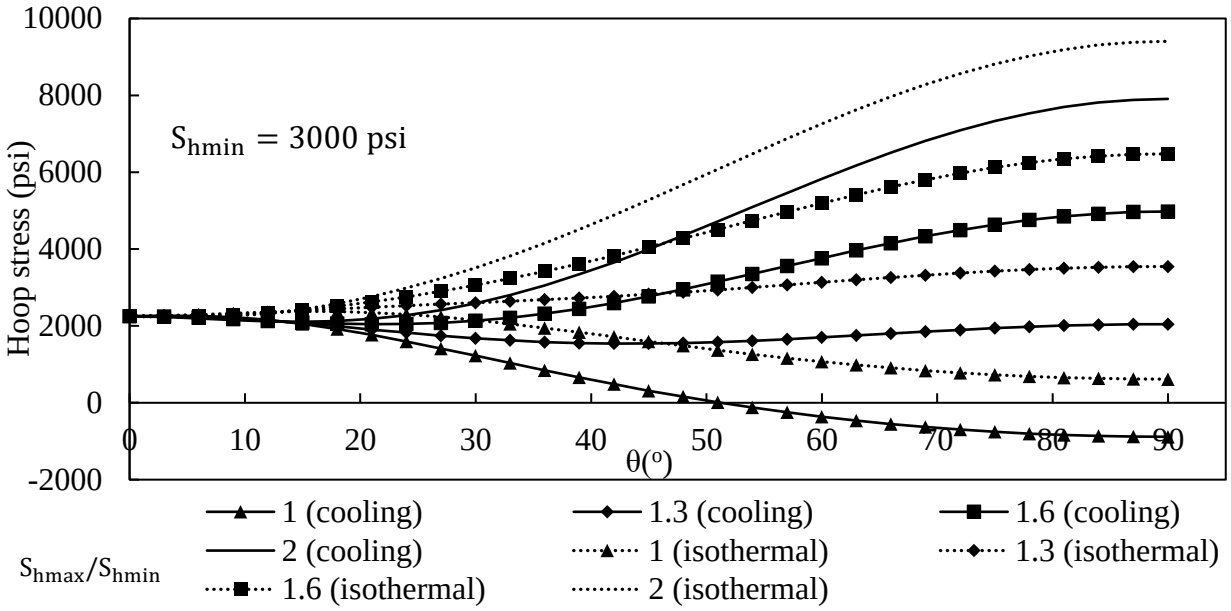

Figure 7.5. Hoop stress along the wellbore wall under the thermal effect (thermo-poroelasticity model).

From Figure 7.6., one can observe a noticeable increase in SIF at the fracture tip when the horizontal stress anisotropy is stronger, which means it is more likely for the fracture to initiate further. In this case, the difference in the SIF under the thermal effect remains the same, as we did not change the temperature condition under the cooling effect.

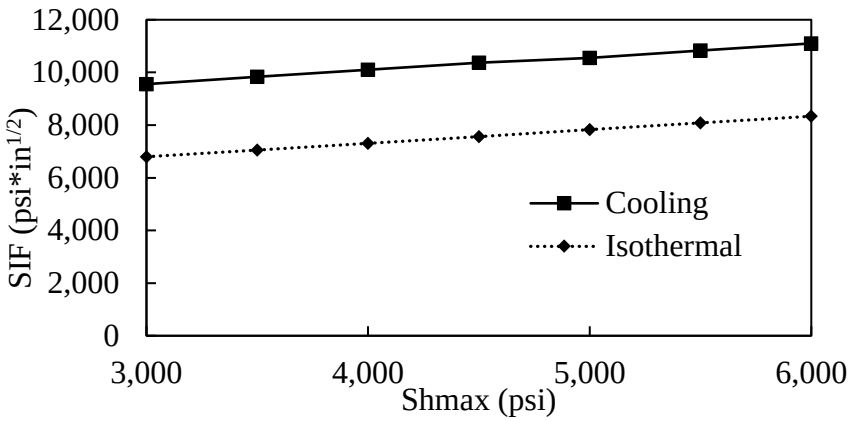

Figure 7.6. SIF under the thermal effect; poroelasticity model with different horizontal stress anisotropies. Minimum horizontal stress is set to 3000 psi.

7.1.4 Parametric Study on Rock Properties (Young's Modulus and Poisson's Ratio)

Young's modulus and Poisson's ratio are two important formation properties. These two parameters also appear in the analytical solution used to determine the fracture pressure under thermal effect. A sensitivity analysis was conducted in this section to investigate the effect of a variety of combinations of Young's moduli and Poisson's ratios of the hoop stress along the wellbore and fracture face. A sensitivity study on Young's modulus was conducted by using the various values of E (E1 = $1x10^6$ psi, E2 = $1.5\ x10^6$ psi, and E3 = $2\ x10^6$ psi) while maintaining a constant Poisson's ratio. The same was done for Poisson's ratio by using a different value of ν (ν1 = 0.2, ν2 = 0.25, and ν3 = 0.3) as Young's modulus remained constant. The results displayed in Fig.10 show that thermal stress induced along the wellbore is strongly influenced by Young's modulus but is less affected by Poisson's ratio. The results are shown in Figure 7.7a). also display that tensile stress might occur on the wellbore when Young's modulus is high, which indicates a high probability of further instability on the wellbore, besides the risk of fracture re-initiation.

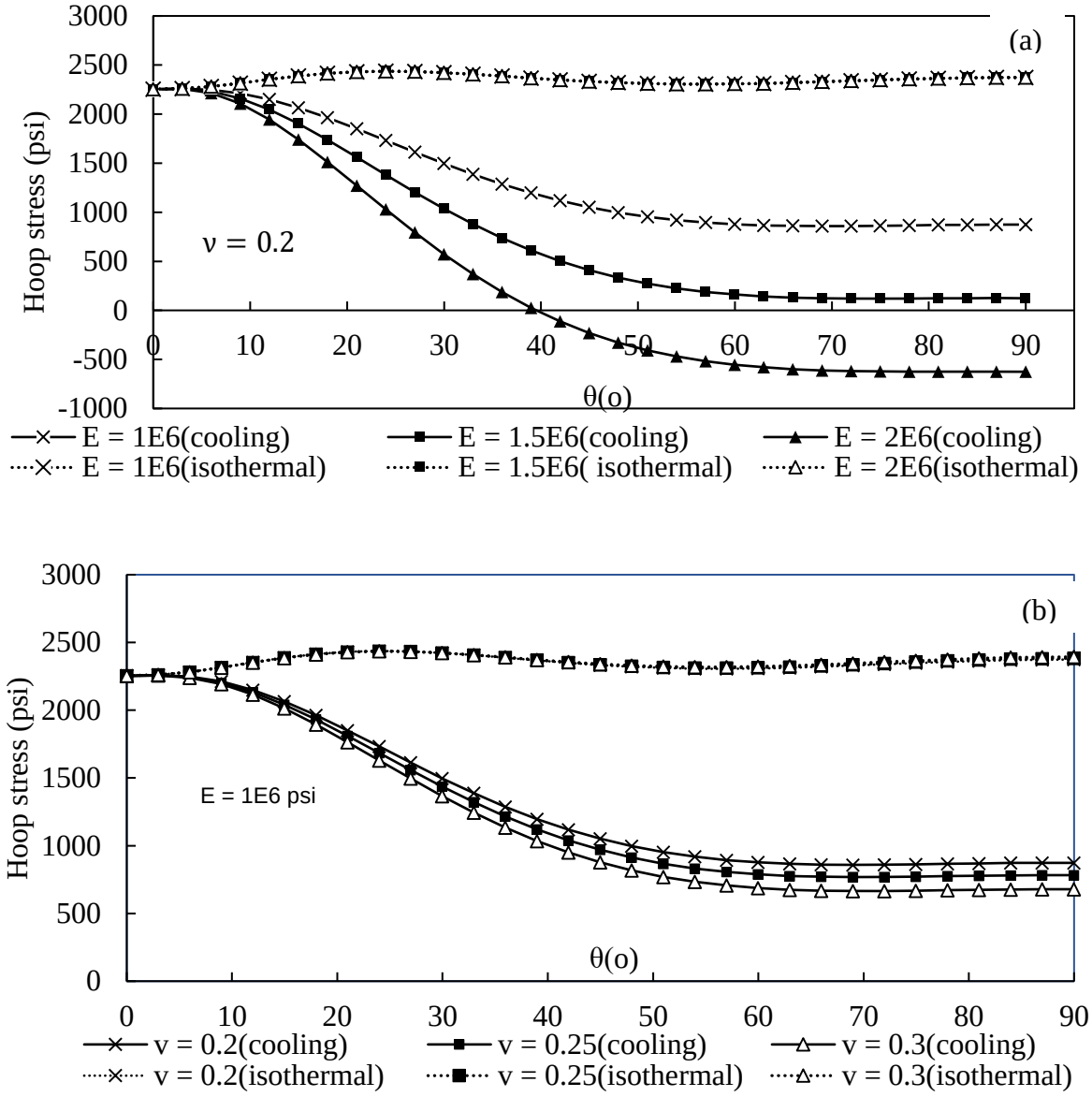

Figure 7.7. Hoop stress along the wellbore wall under the cooling effect with different a) Young's moduli and b) Poisson's ratios.

In previous studies, to find the analytical solution of the SIF at the fracture tip for a fracture that extends from the wellbore, Young's modulus and Poisson's ratio were not included in the calculation. Owing to the consideration of the thermal stress, the two parameters need to be taken into account. The results displayed below in Figure 7-8 indicate an apparent increase in the tensile

stress at the fracture tip when Young's modulus is increased. The effect of Poisson's ratio, however, is minimal.

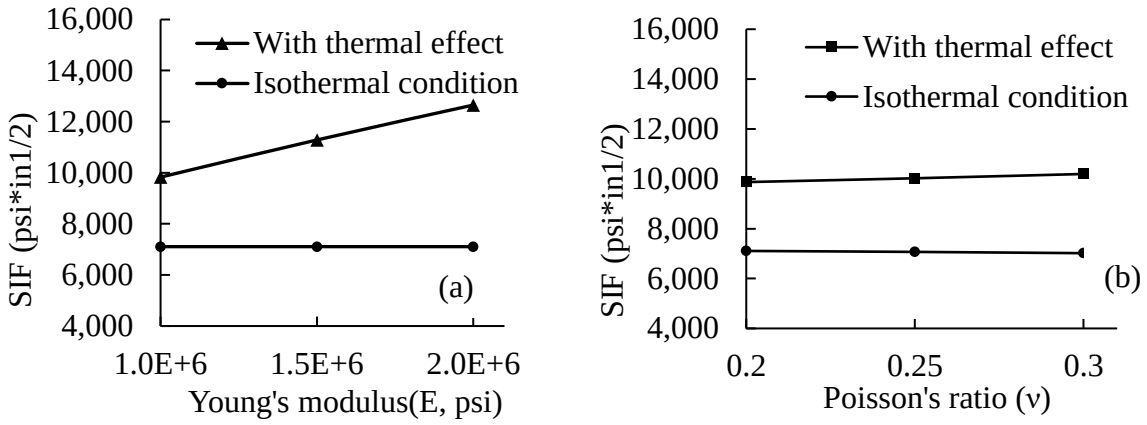

Figure 7.8. SIF under the formation cooling effect for (a) changing Young's moduli (constant Poisson's ration of 0.2), and (b) changing Poisson's ratio (constant Young's modulus of 1E6 psi), thermo-poroelasticity model.

7.1.5 Parametric Study on Fluid leak-off (formation permeability)

Severe lost circulation can occur when drilling through a formation with a narrow mud window. The rate of drilling fluid loss into the formation depends on a variety of parameters, including the permeability of the rock, filter cake building-ups, differential pressure, and the presence of fractures on the wellbore. Depending on different fluid leak-off rates, convective heat transfer induced by cold fluid invasion is also strongly altered. This study uses a predetermined formation permeability to control the fluid leak-off through wellbore wall and fracture surface to study the degree of fluid loss on thermal stress.

As illustrated in Figure 7.9a)., an increase in the rock permeability did not result in a considerable change in the hoop stress along the wellbore under either isothermal conditions or

the cooling process of the wellbore. Under the isothermal condition, hoop stress is not changed with formation permeability.

Analysis of the SIF confirmed the previous observation that fluid leak-off does not have a high impact when the thermal effect is not considered. When the cooling process comes into play, the fluid leak-off rate can have a significant effect on the fracture tip stress state. According to Figure 7-9b), the SIF can be continuously elevated by an increase in the fluid leak-off rate.

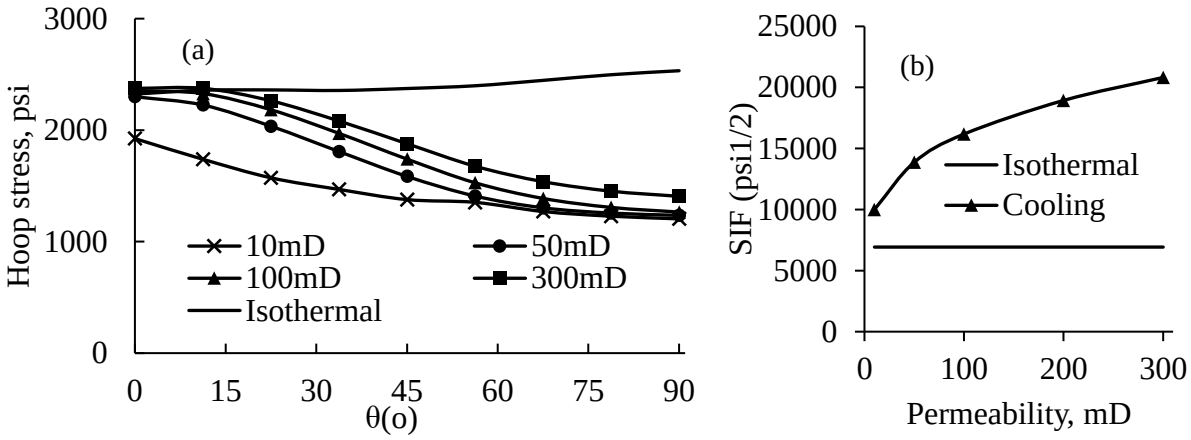

Figure 7.9. a) Hoop stress along the wellbore wall under the cooling effect and b) SIF with different formation permeability

7.2 Statistical analysis: contribution of the individual parameter to thermal effect with unbridged fractures

Four main parameters related to the induced thermal stress and cooling effect on fracture tip are studied in the last section, including formation permeability, Young's modulus, Poisson's ratio, and wellbore temperature. Besides the individual effect of these parameters on SIF, another aspect that interest the author is to measure and compare their overall contribution to SIF and the possibility of fracture re-initiation during formation cooling process. Analysis of Variance (ANOVA) Test is a statistical technique that can be used to quantitatively assess the influences of

the independent parameter on a consequential change of a dependent variable, SIF, in our case. This method is originally used to compare the potential difference among group means by calculating the variances of dependent variable caused by individual parameters. ANOVA Test has different purposes of usage depending on the number of independent variables that could potentially explain the variance of the dependent variable. One-way ANOVA test can be used to test whether different groups of data have similar distribution based on their means according to only one variable. Two or N-way ANOVA study the variance of a data-set related to multiple variables. N-way ANOVA Test can be used to determine whether a group of data differs concerning each of the several targeted variables.

In this study, the author uses N-way ANOVA Test to examine whether a change of each parameter can cause severe variance in SIF value, in another word, can be most influential. N-way ANOVA Test was conducted with the input data from Table 7-1, which collects simulation results of SIF of different lost circulation scenarios in the last section. Effect of wellbore pressure is also included here as another principle factor that controls the SIF and fractures re-initiation. The value range of wellbore pressure is set to be 1*Smin to 2*Smin, which is 3000psi to 6000psi. The primary condition to conduct an effective ANOVA Test is to involve all major parameter that is relevant to the change of SIF. The omission of essential factors can mislead the application of ANOVA Test in practical work. A majority of downhole drilling-related parameters and formation conditions can be accounted for by the parameters selected for the ANOVA Test in this study. Wellbore pressure is an indication of the downhole mechanical conditions caused by ECD, drill string movement, and other abnormal drilling activity. Formation permeability is the major consideration of formation that controls fluid loss into the formation. It is also a major cause of formation temperature due to convective heat transfer. Young's Modulus and Poisson's ratio

decides the formation mechanical properties, and wellbore temperature specifies the difference between wellbore temperature and initial reservoir temperature. In conduction of ANOVA test, one important process is to determine a reasonable range of value for each parameter. Rock properties in this section are chosen to represent a regular sandstone. Rock permeability changes from 10 mD to 300 mD, Young's Modulus changes from 1.45E5 psi to 3E6 psi, Poisson's ration from 0.1 to 0.3.

Table 7.1. Inputs for N-way ANOVA test: parameters and SIF.

Wellbore pressure	Rock permeability	Young's Modulus	Poisson's ration	Wellbore temperature	SIF
4000	100	1.00E+06	0.10	120	1.61E+04
4000	100	1.00E+06	0.20	120	1.62E+04
4000	100	1.00E+06	0.30	120	1.62E+04
4000	100	1.45E+05	0.2	120	8.91E+03
4000	100	1.00E+06	0.2	120	1.62E+04
4000	100	2.00E+06	0.2	120	2.08E+04
4000	100	3.00E+06	0.2	120	2.38E+04
4000	100	1.00E+06	0.2	120	1.62E+04
4000	100	1.00E+06	0.2	80	1.89E+04
4000	100	1.00E+06	0.2	150	1.21E+04
4000	10	1.00E+06	0.2	120	1.00E+04
4000	50	1.00E+06	0.2	120	1.39E+04
4000	100	1.00E+06	0.2	120	1.62E+04
4000	200	1.00E+06	0.2	120	1.89E+04

(table cont'd.)

Wellbore pressure	Rock permeability	Young's Modulus	Poisson's ration	Wellbore temperature	SIF
4000	300	1.00E+06	0.2	120	2.08E+04
4000	0	1.00E+06	0.2	80	1.19E+04
4000	0	1.00E+06	0.2	115	9.97E+03
4000	0	1.00E+06	0.2	150	8.49E+03
3000	0	1.00E+06	0.2	120	4.80E+03
4000	0	1.00E+06	0.2	120	9.50E+03
5000	0	1.00E+06	0.2	120	1.40E+04
6000	0	1.00E+06	0.2	120	1.86E+04

Table 7.2. summarizes the P-value report from N-way ANOVA test. P-value of each variable indicates the significance of individual parameters within their chosen range to the overall variance of SIF. The smaller P-value a parameter gives the more severe SIF response to the change of this parameter, the more important it is. Generally, when P-value of a variable is less than 0.05, engineers consider this variable as having a substantial influence on SIF. As shown in Table 7.2., wellbore pressure, rock permeability and Young's Modulus gives the P-value far less than the 0.05 threshold. This indicates that wellbore pressure alone can contribute dramatically to the change of SIF. Fluid leak-off into formation controlled by formation permeability is also significant due to formation cooling effect. The increase of fluid loss should thus be a primary consideration that poses the risk of fracture instability when a large temperature difference exists between wellbore and reservoir. Young's Modulus is another major contributor to SIF fluctuates. With a normal range of value from 1.45E5 to 3E6 psi, Young's Modulus has a P-value of less than 0.0001 that signals a sufficient influence. On the other hand, wellbore temperature surely affects thermal

stresses around fracture tip with P-value of 0.0031. This means the temperature contrast between wellbore and reservoir, varies from low to high, has a certain degree of influence, yet not significantly, on SIF change due to thermal stress. However, the importance of wellbore temperature should not be underestimated since it is the source of thermal stress and the reason why other factors can affect SIF so much. Among the parameters tested in this study, Poisson's ratio has the least effect on the thermal effect induced around fracture tip.

Table 7.2. The output of the N-way ANOVA Test

Source	DF	Sum of Squares	Mean Square	F Value	Pr > F
Model	5	446098930.7	89219786.1	42.54	<.0001
Error	16	33553845.6	2097115.4		
Corrected Total	21	479652776.3			

Source	DF	Type I SS	Mean Square	F Value	Pr > F
Wellbore pressure	1	5.06E+07	5.06E+07	24.14	0.0002
Rock permeability	1	2.29E+08	2.29E+08	109.26	<.0001
Young's Modulus	1	1.41E+08	1.41E+08	67.22	<.0001
Poisson's ration	1	4.13E+03	4.13E+03	0	0.9651
Wellbore temperature	1	2.54E+07	2.54E+07	12.1	0.0031

Sum of Squares in the output gives the squares of deviation of an actual value from the means of predicted value when the current parameters as a predictor. It explains the contribution of each parameter to the variance of the dependent variable, SIF. The higher sum of the square a parameter

has, the more relevant this parameter will be to the SIF. Sum of Square can be expressed in percentage of the total sum of the square as showed in Figure 7.10. Formation permeability accounts for the 51% of the total SIF change when formation cooling is under consideration, which is the highest among all parameters included in the test. Wellbore pressure is also significant with 11% of the contribution. Change of wellbore temperature contributes to 6% of the SIF change. Young's Modulus is responsible for 32% of the SIF change. Poisson's Ration has the lowest percentage, less than 1%. The results in this section can be especially useful when engineers prioritize the consideration of varies parameters to assess the deterioration of lost circulation, especially when high fluid leak-off rate and temperature difference exists simultaneously.

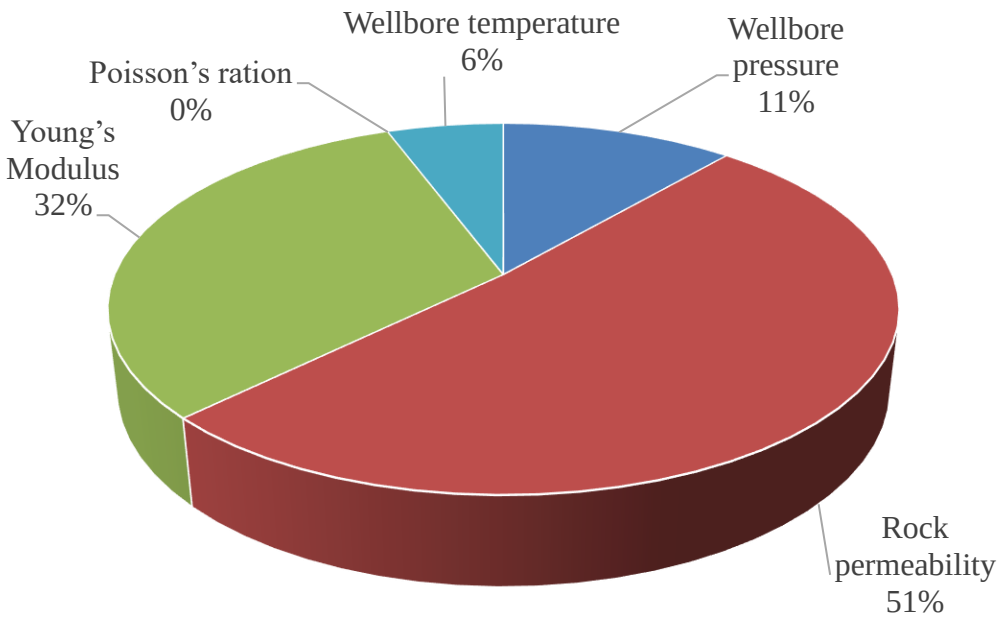

Figure 7.10. The individual contribution of each parameter in percentage

Regression analysis is then conducted subsequently to obtain a predicting model of SIF with the normal rage of parameters. From the plot of the earlier lost circulation simulation, between SIF and each of the important parameters, approximately linear relationships can be observed, leading

to the linear model as our primary consideration. The ANOVA test implies that formation mechanical properties have negligible influence on the variance of SIF under formation cooling process. The linear model is only tested between SIF and leak-off rate, wellbore pressure, and wellbore temperature. The results of linear regression are shown in Table 7.3.

Table7.3. The output of the linear regression test

Source	DF	Sum of Squares	Mean Squares	F Value	Pr > F
Model	5	446098930.7	89219786.1	42.54	<.0001
Error	16	33553845.6	2097115.4		
Corrected Total	21	479652776.3			

Root MSE	1448.142	R-Square	0.93
Dependent Mean	14657	Adj R-Sq	0.9082

Parameter	Estimate	Standard Error	t Value	Pr > |t|
Intercept	-3303.74	4127.2612	-0.8	0.4352
Wellbore pressure	4.274083	0.61093	7	<.0001
Rock permeability	43.40158	4.31083	10.07	<.0001
Young's Modulus	0.005092	0.00062	8.24	<.0001
Wellbore temperature	-71.328	20.50648	-3.48	0.0031

The general prediction model of SIF is provided by the following equations:

$$SIF = -3303 + 4.27 * P_{wf} + 43.40 * \rho + 0.005 * E - 71.38 * T_{wf} \quad (7\text{-}1)$$

The test for the overall linear regression analysis outputs F-value = 54.93 and Pr > F less than 0.0001, confirms that the selected model predictor have a significant response on SIF. The value of R-Square is used to evaluate how much of the actual calculated SIF can be explained by the predicted SIF from the linear model. It measures the goodness-of-fit for linear regression, but it can be misleading for multivariate analysis. Adjusted R-Square is used to compensate for this error, and it gives a value of 0.90, showing a strong predicting power of this linear model.

7.3 Thermal effect on pre-existing fractures with WBS implementation

7.3.1 Comparison between thermoelasticity and thermoporoelasticity (with and without pore pressure)

This section Influences of WBS implementation on thermal effect induced during fluid invasion have been explained in detail in Chapter 5 and Chapter 6. Figure 7.11 gives the trend of SIF change during WBS when poroelasticity and thermoporoelasticity model is adopted into FE study. Fluid leak-off rate is pre-set to be zero in Chapter 6 for the preliminary validation with the analytical solution, which has no fluid leak-off consideration. The figure shows that when poroelasticity is taken into accounts, SIF is overall higher than the result from pure linear elasticity. The decline of SIF as plugging position moves to fracture mouth shows similar trend showed in thermoporoelasticity. It also has a gentle decline followed by a more dramatic falling. If we consider linear elasticity model to represent low permeability formations and poroelasticity model for formations with considerable permeability and porosity. This observation implies that WBS implementation in permeable formation is less effective than low permeability formations when similar fracture geometry and loading condition is under consideration. Comparing to linear elasticity and thermoelasticity simulation, thermal effect on SIF in this section is rather uniform, nor differing much with plugging position.

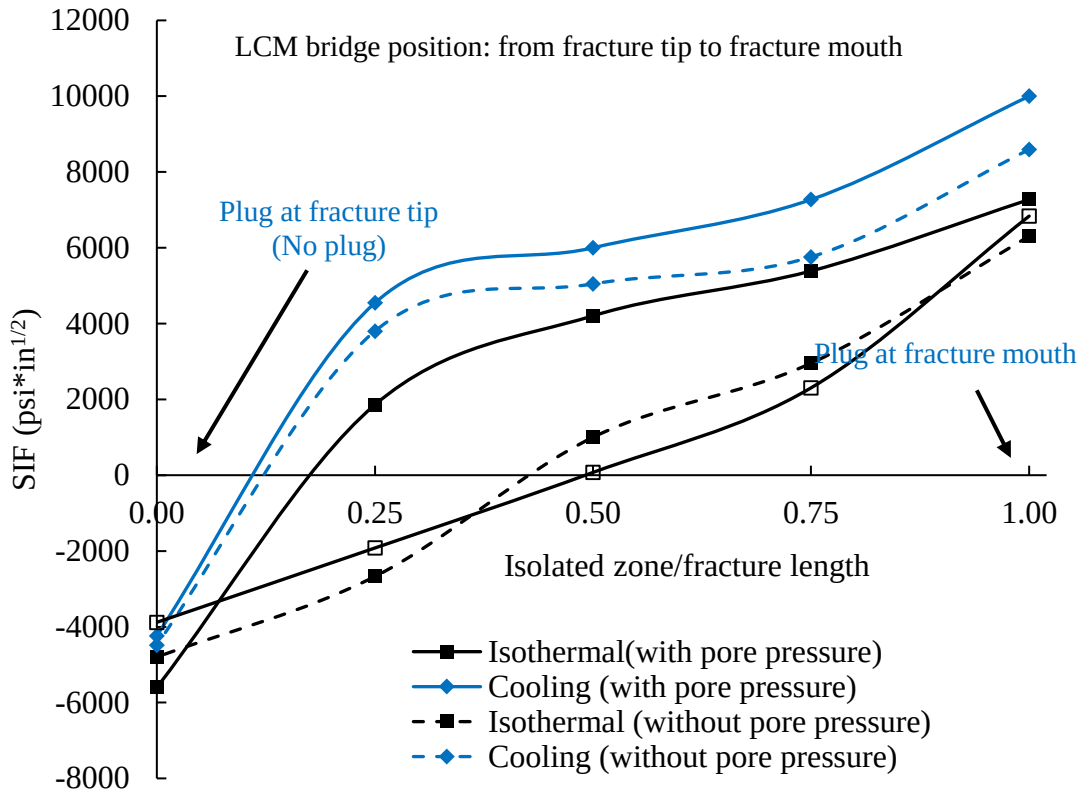

Figure 7.11. SIF at fracture tip with LCM bridging the fracture at different positions, with and without considering wellbore cooling effect. Consider poroelasticity and pore pressure in the formation.

7.3.2 Thermal effect on SIF with WBS implementation with different fluid leak-off rate

Zero fluid leak-off rate set-up utilized in Section 7.3.1 benefits the simplification of the simulation for the preliminary discussion, but it doesn't comply with the assumption of uniform temperature boundary inside fracture space. When inside fluid fracture remains static, fluid temperature yields to the temperature of surrounding formation. It can hardly maintain at the constant wellbore temperature during simulation, as assumed in modeling methodology of this study. The constant wellbore temperature assumption is most effective when fracture fluid keeps being fed by wellbore fluid as fluid loss happens. Thus, in this section, a sensitivity analysis on

fluid leak-off rate is carried out to further clarity the cooling effect on thermal stress and fracture re-initiation.

Figure 7.12., summarizes the SIF under cooling effect at different plugging position, with different fluid leak-off rate applied. As suggested by the case of simply lost circulation earlier without fracture plugging, fluid leak-off can dramatically elevate the SIF under cooling effect. The quantitative difference between SIF under isothermal and cooling condition remain relatively stable, despite the different plugging position. The general trend of SIF with a series of fluid leak-off rate presents the same observation as in Section 6.3: formation cooling effect can increase the SIF and weaken the WBS implementation. Another interesting observation is that higher leak-off rate leads to lower SIF when the fracture is plugged at the mouth. This indicates that when a fracture is fully plugged, cooling effect act to reinforce the compressive stress state at fracture tip.

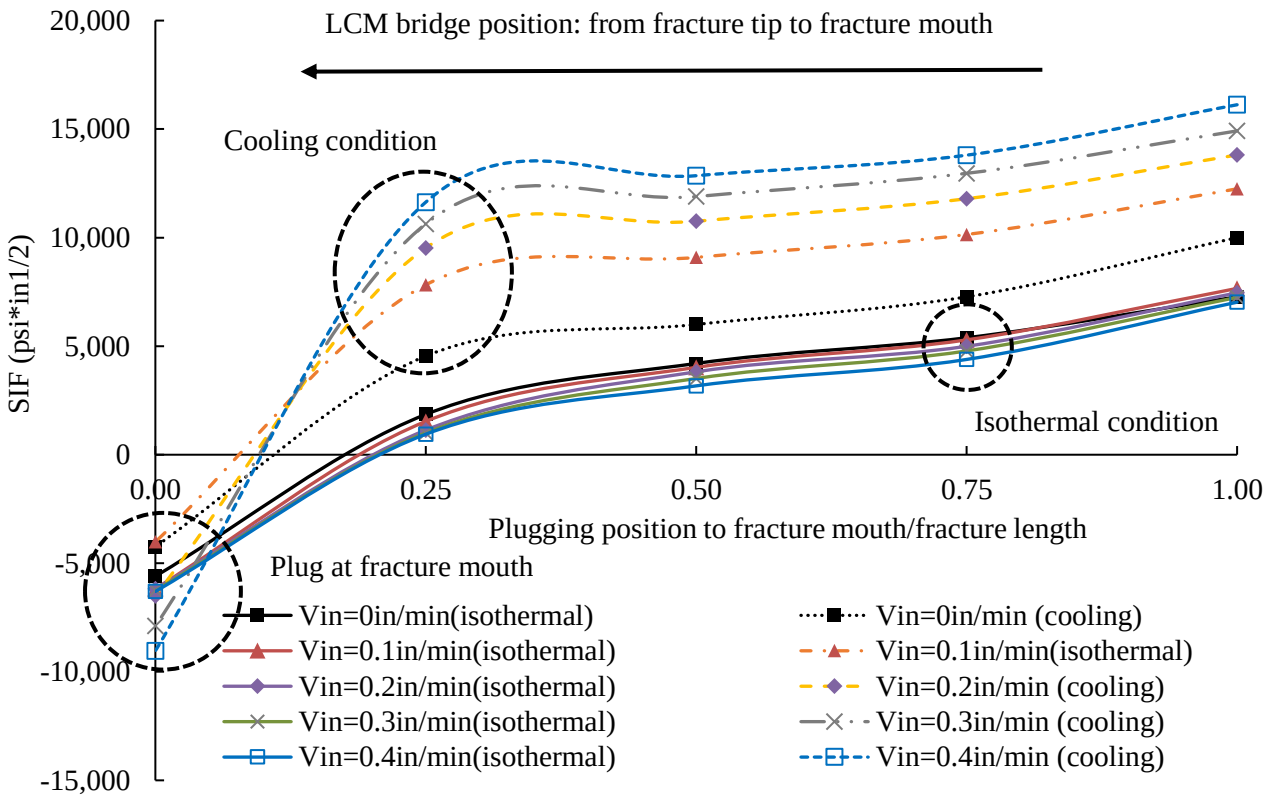

Figure 7.12. SIF at fracture tip with LCM bridging the fracture at different positions, with and without considering wellbore cooling effect. Consider poroelasticity and pore pressure in the formation.

7.3.3 Thermal effect on pre-existing fractures during WBS with inner filter cake build-up

Figure 7.13. summarizes the simulation results of SIF at fracture tip with different inner filter cake permeability. When inner filter cake permeability equals the formation permeability (100 mD), it is the equivalent of the state when no filter cake is formed, and fluid can leak through fracture surface with no restriction. This yields the maximum cooling effect on SIF due to high fluid leak-off rate. As showed in Figure 7.13., despite the minimal thickness of inner filter cake layer, fluid leak-off and influence of the cooling effect of fracture initiation can still be strongly undermined when sufficiently low permeability created in this layer. However, without considering the mechanical strength of the inner filter cake, this mechanism can only protect

fracture tip from the influence of high fluid leak-off rate. Fracture tip is still exposed to high wellbore pressure and low fluid temperature.

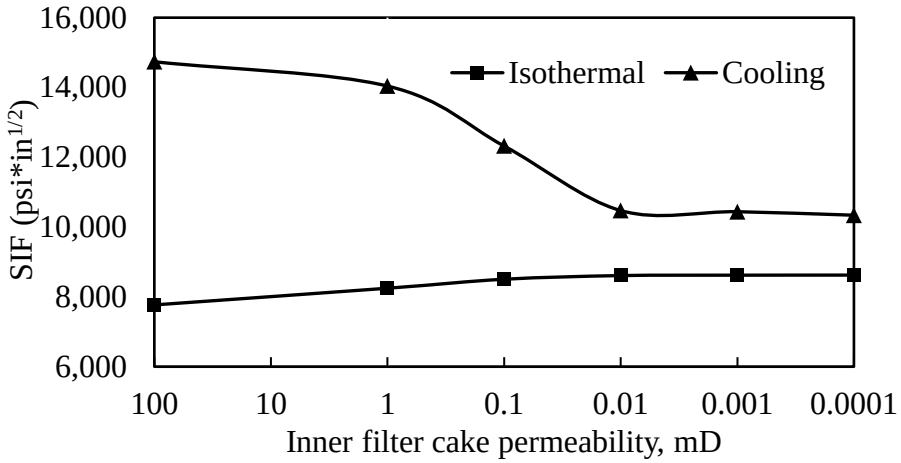

Figure 7.13. SIF with different inner filter cake permeability, with and without considering wellbore cooling effect.

Chapter 8. Laboratory Experiments to Explore Wellbore Temperature Control Using Thermal Insulating Materials

Besides the thermal property data presented in the Methodology section, this study also designs a series of experiments to explore the reasonable range of those properties and temperature set-ups of formation and wellbore fluid. The author considers the necessity of such experiment in two ways. Simulation of thermal stresses in near wellbore formation relies on the input of temperature parameters and thermal properties of all relevant materials including thermal conductivities and specific heat. Among those, thermal properties of drilling fluid are directly related to the temperature distribution in wellbore besides drilling operations. Filter cake formed on wellbore by drilling fluid of different type can also have a positive or negative side effect on heat exchange process in the wellbore (Teodoriu et al., 2016, Ichim et al. 2017). Thermal conductivities and specific heat, especially for drilling fluid, varies with different drilling fluid additives. More importantly, the variation of fluid properties due to change in its component can have an overall influence on the temperature distribution in the wellbore. During drilling practices, large quantities of fluid additives are added into a fluid such as light weight material for underbalanced drilling, LCMs et al. These materials can have a significant influence on the properties, especially the thermal properties, of drilling fluid. Fluctuation of wellbore temperature caused by the use of these materials is also worth studying. These are all important factor to consider when it comes to the input of thermoporoelasticity modeling established in this study. Thus, although thermal properties in the simulation are fixed as the same as earlier studies, it's still strongly recommended to explore the range of possible thermal properties values according to specific drilling fluid types.

Secondly, the efforts to study the thermal properties of one leads to the possibility to control wellbore temperature with either physical or chemical methods. Engineers have striven to mitigate the negative effect of temperature on both reservoir rock and wellbore fluid. Other than induced

thermal stress induced in near wellbore region, fluid properties change during temperature fluctuation also concerns the petroleum engineers. Unlikely to control heat loss of formation, most works in this area were conducted to improve fluid endurance to high temperature. Other researchers managed to identify factors that influence temperature increase in the wellbore, including drilling-related parameters like circulation rate and wellbore dimensions (Maury et al. 1995, Gonzalez et al. 2005). A preliminary experiment was also performed trying to heat up the bottom hole by adding chemical composition in drilling fluid (Hoxha, 2016). Despite these efforts, potentials of managing fluid properties, thermal properties especially, have not been fully recognized yet.

Given these two considerations, a series of experiments are conducted in Chapter 8 at the end of this thesis to explore the possibility of wellbore and reservoir rock temperature control by using drilling fluid additives with specialized thermal properties. Preliminary experiments were performed firstly, and the results were implemented in mathematical modeling to examine the wellbore and formation temperature. The logic is to reduce the thermal exchange between the wellbore and circulating fluid to a minimum so their temperature won't be influenced by each other. Fluid additives are of interest mostly because some of them have already been applied during drilling for purposes such as mud weight control or fracture plugging. Another advantage regards the convenience of their implementation that needs no interruption of the current drilling process.

Chapter 8 aims to identify the additive that alters the fluid thermal properties most effectively, referred to as thermal insulating additives (TIA). The effect of TIA is in three-fold. First of all, a variation of mud weight will change the mass flow and heat flow process during drilling. Secondly, these additives are expected to change thermal conductivity and heat capacity of drilling fluid. Most importantly, when the relatively high concentration of TIA is used in drilling fluid,

components of filter cake generated during this process could be altered considerably. With the existence of low thermal conductivity components, thermal properties of mud cake will be decreased. These three effects all contribute to the overall temperature profile of wellbore and formation in near wellbore region. Three types of additives are identified for preliminary tests due to their low thermal conductivity: hollow glass bubble or hollow glass sphere (HGS), magma fiber lost circulations materials (LCM), fiberglass, and glass beads. Hollow glass bubble is the most promising materials among them. And applied it into analytical and numerical models to examine its effectiveness in wellbore temperature control.

HGS is small-sized glass bubble with hollow space inside filled with air. With considerably low density, it has been utilized by the industry as a weight reducer during drilling depleted reservoirs with low fracture pressure. Despite its excellent thermal insulating properties, its thermal effect on the drilling process is rarely studied. Other selected materials can also have low thermal conductivities. Magma fiber is a coarse material consist of minerals and other fibrous materials that can be applied to plug the fractures and mitigate lost circulation. It is fully soluble in water or water-based drilling fluid. Fiber glass with shorter length can also be added into drilling fluid for the same purpose. Glass beads are solid glass sphere that is not soluble in water and with much higher density and strength. It is only used in a small amount as a lubricant in drill strings and other bottomhole facilities.

For the first step in this report, a thermal property analyzer was utilized to characterize the effect of these materials on the thermal properties of drilling fluids and filter cakes. This step was specially designed to compare the performance of different materials and identified the additives that could alter the thermal properties of drilling fluid and filter cake most effectively. Thermal properties test results of drilling fluid and filter cake were then collected to be used in the second

step as input to simulate the downhole temperature profiles in the wellbore and surrounding formations. Finally, the most optimized performance of the TIAs on temperature control is evaluated, both as whole mud treatment and locally applied thermal barrier with filter cake.

8.1 Preliminary experiments of drilling fluid and filter cake properties after adding special fluid additives

Experiments were first conducted to characterize the effect of these materials on the thermal properties of drilling fluids and filter cakes. Filter cakes were generated using OFITE filter press (as shown in Figure 8.1a).), Thermal conductivity and specific heat of drilling fluids and filter cakes were tested – samples with and without HGS using TPS500S thermal conductivity analyzer (as shown in Figure 8-1b)). Here drilling fluids were prepared with water and 8% bentonite.

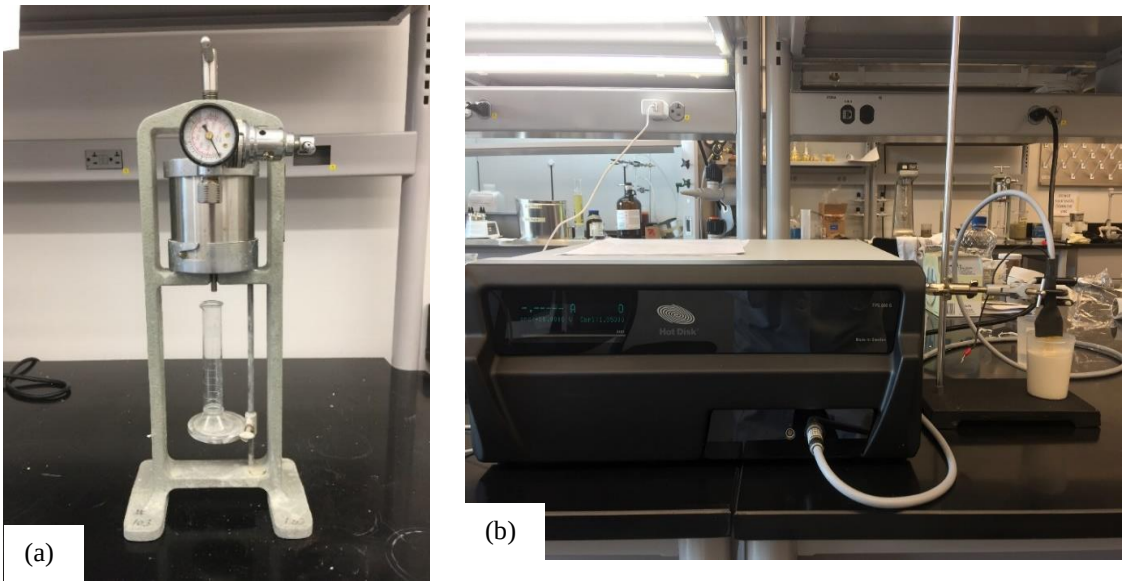

Figure 8.1. (a) OFITE Filter Press used for generating filter cakes and (b) thermal conductivity analyzer – HotDisk TPS500S

8.1.1 Thermal properties test with HGS

In this test, HGS is added into drilling fluid with gradually increasing concentrations up to a maximum value of 42% in volume. Filter cakes samples generated with and without HGS are shown in Figure 8.2. Table 8.1. and 8.2. shows thermal properties of drilling fluids and filter cakes with and without adding HGS. Figure 8.3. and 8.4. summarizes the trend of these properties. The thickness of thermal insulating filter cakes with HGS was measured as 6 mm, comparing to 2 mm for regular filter cake with 8% bentonite.

Figure 8.2. Filter cake generated by low gravity solids drilling mud without HGS (sample at left), and with a high concentration of HGS (right).

Table 8.1. Thermal properties of drilling fluid with and without adding HGS

Sample type	regular	with 15% HGS	with 30% HGS	with 42% HGS

Density (kg/m3)	1039	960	880	767
Thermal conductivity (W/m. k)	0.69	0.58	0.47	0.40
Specific heat, mass (J/kg. K)	3742	3689	3093	3035

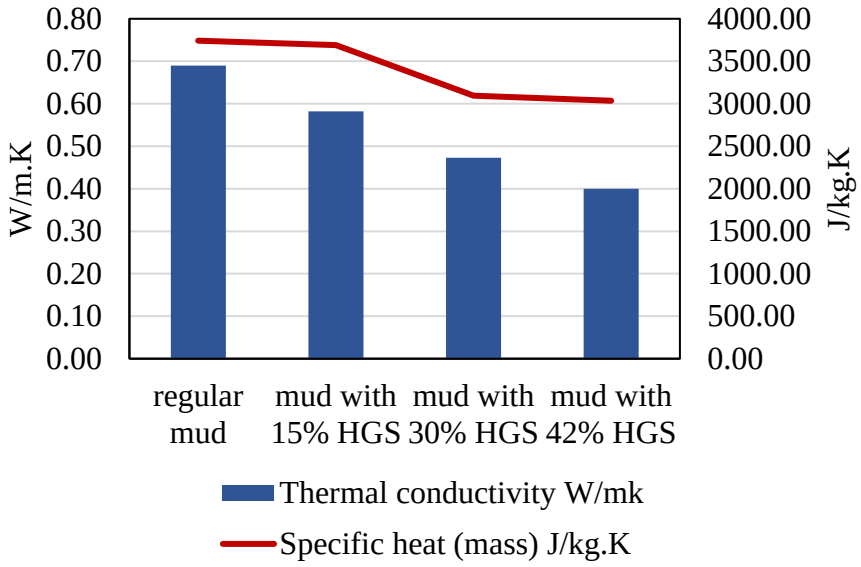

Figure 8.3. Change of thermal properties of drilling fluid by adding HGS

Table 8.2. Thermal properties of filter cake with and without adding HGS

Sample type	regular	15% HGS	30% HGS	42% HGS
density (kg/m3)	1772.00	995.00	710.00	700.00
Thermal conductivity (W/m. k)	0.62	0.41	0.36	0.31
Specific heat (J/kg. K)	2579.01	2703.52	2692.00	2757
Specific heat (MJ/m^3.K)	3.89	3.54	2.72	2.33

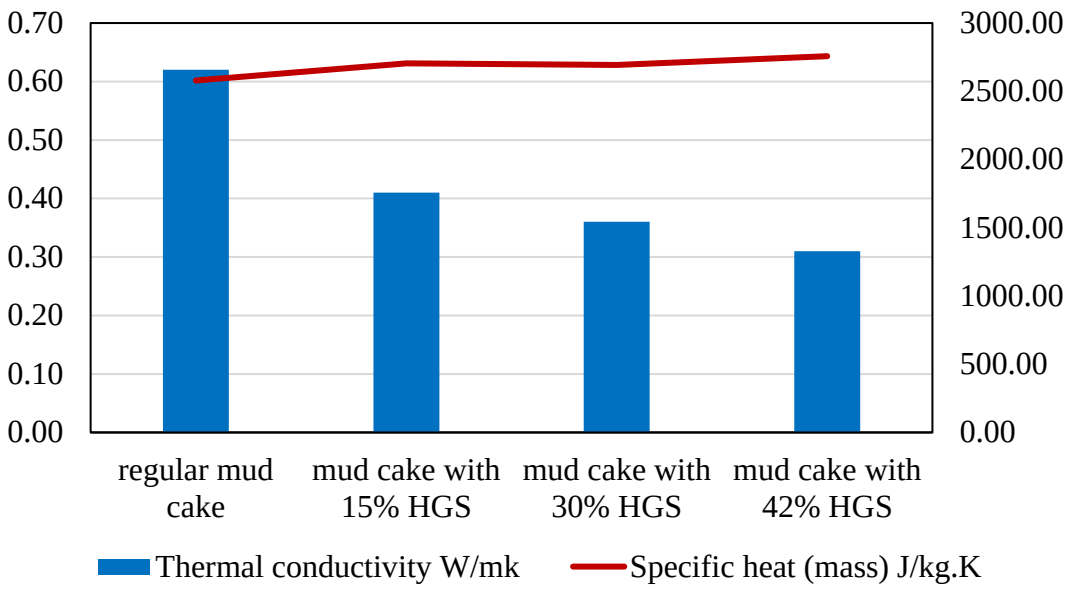

Figure 8.4. change of thermal properties of filter cake by adding HGS

8.1.2 Thermal properties test with magma fiber LCM

Use of magma fiber in mud is measure by kg/m3 or lb/bbl (1lb/bbl = 2.85 kg/m3). Normal range of magma fiber concentration is 6-84 kg/m3 (2-30 lb/bbl). Here magma fiber was added with a relatively high concentration to test its thermal effect when used in a large amount. As shown in the results Table 8-3 below, magma fiber has negligible effect on thermal properties of fluid and filter cake.

Table 8.3. Thermal properties of drilling fluid and filter cake with and without adding magma fiber

Sample type: drilling fluid

Additive concentration	17.5 lb/bbl	35 lb/bbl
Thermal conductivity (W/m. k)	0.69	0.67
Specific heat, mass (J/kg. K)	3789	3850

Sample type: filter cake

Additive concentration	17.5 lb/bbl	35 lb/bbl
Thermal conductivity (W/m. k)	0.61	0.64
Specific heat, mass (J/kg. K)	2611	2701

8.1.3 Thermal properties test with fiberglass

Fiberglass is a commonly used fibrous material that can improve cement strength and minimize cement loss through fractures on the wellbore. When the size of fiberglass is small enough, this material can also be applied into drilling fluid in relatively large quantity as an LCM. 3mm short fiberglass has recently been produced for the application of LCM. The thermal conductivity of fiberglass can be as low as 0.04 – 0.2W/m. K, which is the reason why it is selected. Unlike powdered HGS, fiberglass cannot be dissolved into the fluid. Normal use of fiberglass in cement is only 2 lb/bbl. Here it is used as an additive in the mud with much higher concentrations: 5% in volume (17.3 lb/bbl) and 10% in volume (34.1 lb/bbl) of fiberglass were used. Thermal conductivity and specific heat were then tested for both mud and filter cake. According to the test results in Table 8.4., fiberglass can reduce the thermal conductivity of mud and filter cake, but the influence is very limited.

Table 8.4. Thermal properties of drilling fluid with and without adding fiberglass

Sample type: drilling fluid

Additive concentration	17 lb/bbl	34 lb/bbl
Thermal conductivity (W/m. k)	0.65	0.62
Specific heat, mass (J/kg. K)	3730	3685

Sample type: filter cake

Additive concentration	17 lb/bbl	34 lb/bbl
Thermal conductivity (W/m. k)	0.61	0.58
Specific heat, mass (J/kg. K)	2736	2668

8.1.4 Thermal properties test with glass beads

The concentration of glass beads is also measured by weight. It is usually used in mud system as a lubricant to reduce friction of downhole equipment. Due to its high strength and density, glass beads are usually used in a low concentration up to 5.7 lb/bbl. Without that limitation in this study, we increase the use it to a much higher concentration to test the influence of glass beads in an extreme situation. From the results in Table 8.5., although used in a very high concentration, glass beads still have minimal effect on mud and filter cake properties.

Table 8.5. Thermal properties of mud

Sample type: drilling fluid

Additive concentration in drilling fluid	80 lb/bbl
Thermal conductivity (W/m. k)	0.67
Specific heat, mass (J/kg. K)	3708

Sample type: filter cake

Additive concentration in drilling fluid	80 lb/bbl (80 g/350mL)
Thermal conductivity (W/m. k)	0.63
Specific heat, mass (J/kg. K)	2705

8.2 Modelling temperature profile in the wellbore and surrounding formation.

Among three candidates with low thermal conductivity, HGS has the strongest effect on thermal properties of drilling fluid and filter cake. Thus HGS is the optimal candidates of TIA. The thermal insulating effect of this selected TIA was then evaluated through temperature profile modeling within the wellbore and formations. Experimental data regarding HGS were implemented as input parameters. TIA alters overall wellbore temperature when used in the whole mud treatment. When applied in only a short period, especially when used as an LCM pill, components of filter cake formed at this period can be significant change. Wellbore temperature might remain unchanged, but the surrounding formation might be protected by the newly formed filter cake made by the TIA pill.

8.2.1 TIA used as whole mud treatment

In this scenario, measured densities and thermal properties of drilling fluid were used to calculate convective heat transfer coefficients during mud circulation. Thermal conductivities of

filter cakes were used to obtain the overall heat transfer coefficient through wellbore wall. These two coefficient are two deciding factors of wellbore temperature distribution. The calculation assumes cased hole for the upper section of the wellbore (no filter cake buildup and heat transfer through casing and cement) and openhole for lower sections of the wellbore, as is showed in Figure 8.5. U_p,U_{a1} U_{a2} represents overall heat transfer coefficient through drilling pipe, wellbore wall with casing, and wellbore wall with filter cake respectively.

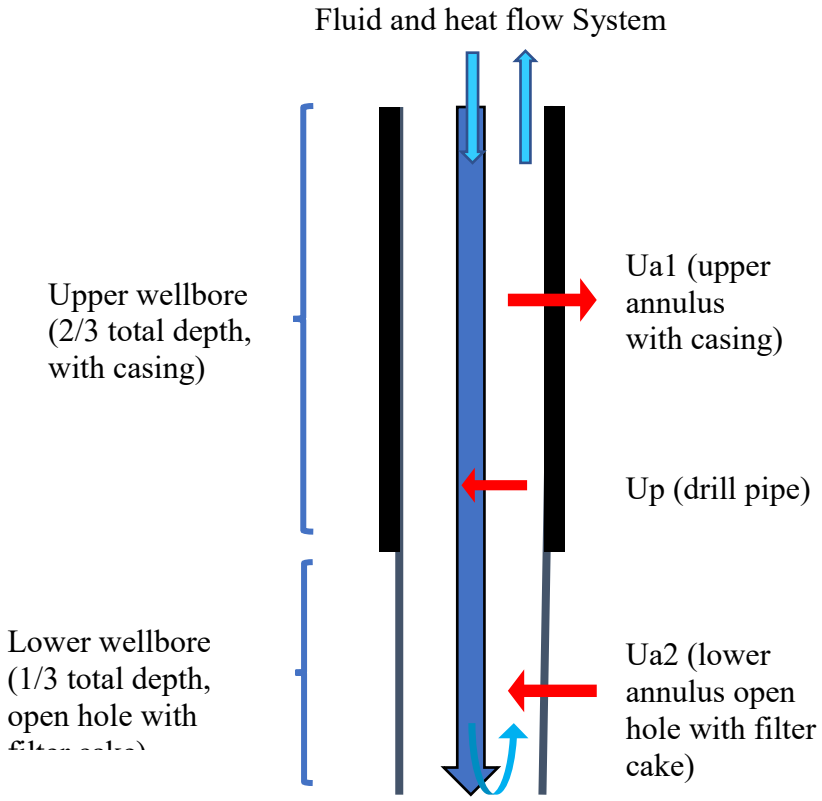

Figure 8.5. Mud circulation and heat transfer system while drilling.

Table 8.6. Input parameters for fluid and heat flow simulations taken from previous literature

Parameters	Value(field unit)	Value (SI)
Model length	400 in	10 m
Wellbore radius	4.25 in	0.1075 m
Rock Permeability	100 mD	9.8692E−14 m^2
Rock Porosity	0.3	0.3
Rock density	0.0979 lbm/in^3	2709.9 kg/m^3
Rock thermal conductivity	1.15 Btu/(ft*F*hour)	2 W/(m*K)
Rock thermal expansion coefficient	1.6E-5 F^{-1}	3 E−5 K^{-1}
Rock specific heat(heat capacity)	0.19 Btu/(lb/F)	790 J/(kg*K)
Fluid viscosity	23 cP	0.023 Pa·s
Mud thermal conductivity(Kabir ,1996)	1 Btu/(ft*F*hour)	1.7 W/(m*K)
Drilling fluid specific heat(Kabir, 1996)	0.4 Btu/(lb/F)	1673 J/(kg*K)

In Table 8.3. and 8.6., we note differences between thermal properties of drilling fluid from literature compared to the ones from experiments conducted in this project. The differences are partially owning to the relatively simple composition of drilling fluids in our experiments. Previous work has proved the great impact of drilling fluid additives on the thermal properties of drilling fluid (Teodoriu et al. 2016). As a result, more tests are required in the second half of the project to further clarify this finding. For fluid system 1 and 2, the authors assumed HGS only affect thermal properties of filter cakes in each drilling fluid system while thermal properties of whole drilling

fluid system remain the same. For fluid system 3, thermal properties of both drilling fluid and filter cakes follows the measured values in the experiments. Influence of HGS filter cake on overall heat transfer coefficients is presented in Table 8.7.:

Table 8.7. Overall heat transfer coefficients used for calculation of drilling fluid temperature profiles during drilling.

	Base fluid system 1(data from literature)		Base fluid system 2(data from experiments)		Fluid system 3(HGS drilling fluid and HGS filter cake)
Filter cake type	Regular filter cake	HGS filter cake	Regular filter cake	HGS filter cake	HGS filter cake
Thermal conductivity, W/(m*K)	1.7		0.634		0.329
Specific heat, J/(kg*K)	1673		4042		3966
Up, W/(m^2K)	319		178		135
Ua1, W/(m^2K)	198		133		109
Ua2 , W/(m^2K)	131	18	99	16	15

Temperature profiles in annuli are shown in Figure 8.6.; these results were obtained using Kabir's model with parameters from Table 8.6. According to the results, drilling fluid temperature in the annulus is much higher when drilling fluid system one was used, which was anticipated since mud system one is of considerably higher thermal conductivity and specific heat. The effect of a thermal insulating filter cake on mud circulating temperature took place mainly through the decrease in overall heat transfer coefficient in openhole sections. Nevertheless, this reduction of overall heat transfer in wellbore does not result in a significant change to annular temperatures. Bottomhole temperature was reduced by around 8 K after the establishment of thermal insulating filter on open hole section. On the other hand, if one were to compare the bottomhole temperature with fluid system 1 and fluid system 3, a significant temperature difference- over 20 K reduction

can be observed, which indicates significant cooling effect using the thermal properties from mud sample in this study comparing to the thermal properties in previous literature. Additional tests will be performed to justify the results, more tests with different concentration of HGS as well other TIAs candidates will be evaluated.

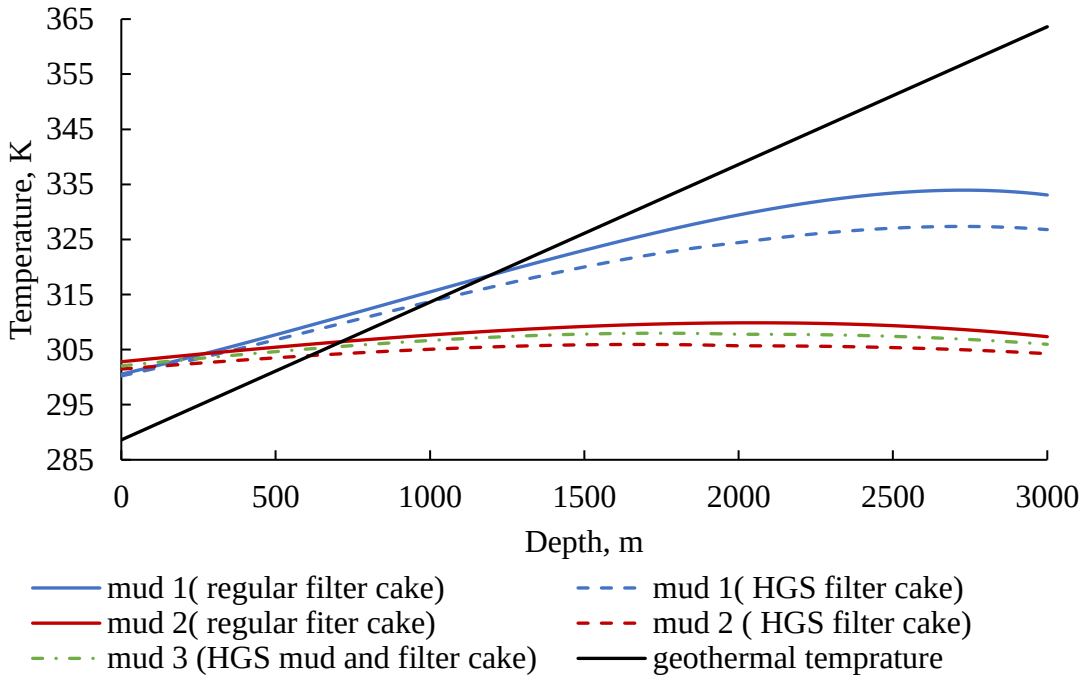

Figure 8.6. Mud circulating temperature in the annulus with different mud systems and filter cakes

8.2.2 Localized thermal insulating filter cake and implication on thermal wellbore strengthening

The second scenario is the application of locally applied thermal barrier as a pill, ultimately the thermal wellbore strengthening that can be achieved by this method. This process can result in the redistribution of formation temperature at a depth of applied thermal barrier while the whole wellbore temperature remains relatively unchanged. Finite element analysis was used, and a 3D wellbore model with filter cake layers was established, as showed in Figure 8.7. To simulate the

effect of a local insulating filter cake, the filter cake layer in the middle was preset to be low thermal conductivity, which neighbors regular filter cakes without HGS.

Temperature distribution in formation rocks at a depth of local thermal barrier was plotted from the interface between filter cake and formation to the internal formation along path 1 and path 2, as showed in Figure 8-7. Path 1 represents scenario a): the formation rock is covered by regular filter cake without the use of HGS. Path 2 represents scenario b): the formation rock is covered by thermal insulating filter cake with the use of HGS. Scenario c) represents low permeability formations like shales, where only heat conduction is considered in the porous media; Scenario d) represents highly permeable formations, heat convection due to fluid leak-off into the formation cannot be neglected.

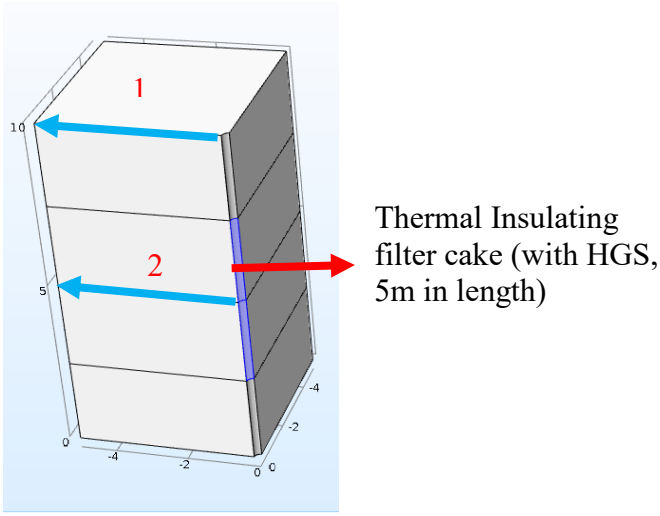

Figure 8.7. Schematic of the wellbore and near-wellbore formation. Heat transmission from wellbore along path 1 and 2. Path one represents the temperature of formation that is covered by regular filter cake without the use of HGS. Path two represents formation that is covered by thermal insulating filter cake with HGS.

The results in Figure 8.8. shows that though reduced from 0.61 to 0.31 W/m.K by using HGS, thermal conductivities of filter cake has minimal effect on formation temperature distribution

around the wellbore. The cooling process of formation is dominated by the fluid invasion. As long as filter cake is built up on wellbore wall as fluid restriction, cooling process can be limited sufficiently, regardless of the thermal properties of the filter cake.

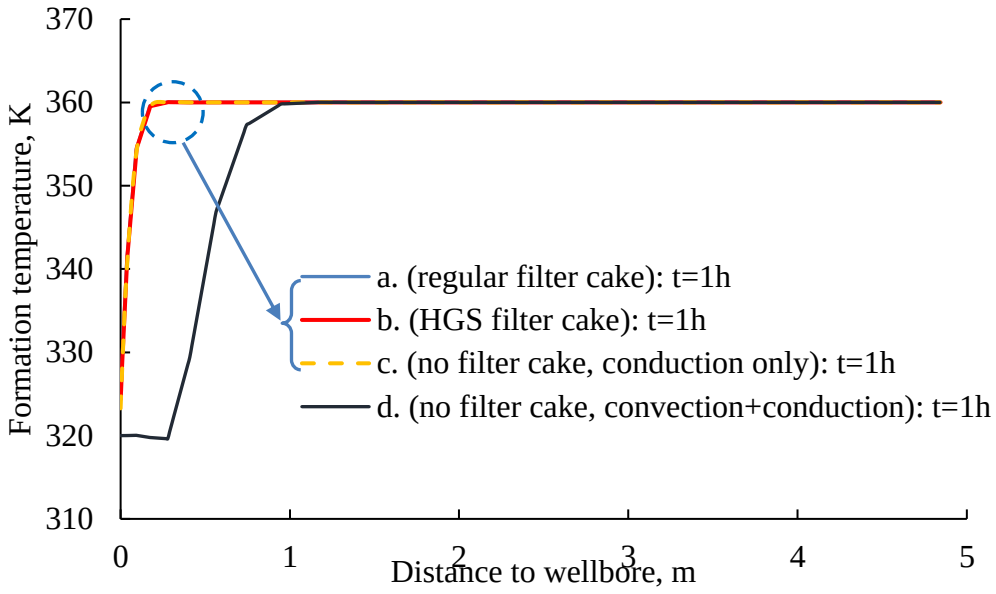

Figure 8.8. Temperature distribution with a) regular filter cake, b) thermal insulating filter cake using HGS, c) no filter cake while considering heat conduction only, d) no filter cake while considering heat convection with fluid invasion and pore fluid flow, in addition to heat conduction. Assuming low permeability of filter cake, no fluid leak-off into formation was allowed when filter cake was generated. Simulation time was set to be t = 1h.

8.3 Discussion of the simulation results.

The Effectiveness of HGS containing mud as whole mud treatment in controlling the temperature inside the wellbore is satisfactory when a high concentration of HGS is used in the mud. In the case study provided in this research, over 20 K of temperature increase in bottomhole temperature at steady state condition is observed when a very high concentration (42% volumetric concentration) of HGS was used. With such as high reduction in mud weight, wells in which this method can be applied is limited without the addition of weighting material or managed pressure

drilling devices. Therefore evaluation should be carefully performed before applying such a method.

On the other hand, HGS containing drilling fluids is not very effective in achieving localized thermal wellbore strengthening by creating filter cakes with low thermal conductivity. Based on case study performed in this investigation, with one hour of circulation after the thermal insulating filter cake was applied, sand face temperature has no obvious difference with regular filter cake.

Chapter 9. Conclusions and Recommendations.

During drilling practices, the temperature change of the surrounding rock, as a consequence of the invasion of mud, has been identified as a vital factor that can cause wellbore instability and severe lost circulation. Nevertheless, most of the relevant research has been conducted in the context of the intact wellbore. There is still a lack of understanding of how the thermal effect influences a wellbore with pre-existing or induced short fractures, which is commonly encountered in lost circulation scenarios. This study carried out a 3D finite element model to simulate the stress redistribution under thermal effect around a wellbore with short fractures. Cold fluid invasion through wellbore wall and fracture surface were utilized as a primary parameter that dominates the local temperature and pore pressure change, both of which were included in the thermo-poroelasticity modeling.

The results of this study lead to the following conclusions:

- As near-fracture formation rock is cooled down by the wellbore fluid, the hoop stress along the wellbore wall decreases. This leads to a lower compressive stress state and a weakened wellbore.
- Owing to the thermal effect created by the reduction of formation temperature, the hoop stress around the tip of a pre-existing fracture also significantly reduces. This indicates that it is likely that a fracture re-initiation (the initiation of pre-existing or drilling induced fractures) will occur as a result of the cold invasion of mud, which can lead to a more severe lost circulation event.
- When a substantial temperature difference exists between the formation rock and wellbore fluid, stress variation is not uniform along the wellbore. Maximum stress reduction along the wellbore occurs at the wellbore with the direction perpendicular to the fracture

extending direction. This signals an increasing possibility of wellbore instability at those points.

- The horizontal stress state is an important parameter that controls the stress state in the near-wellbore region. While the compressive stresses acting on the wellbore wall are intensified by an elevation of S_{hmax}, the SIF analysis shows that the fracture tip sustains higher tensile stress and experiences a higher risk of fracture initiation.
- Of the two most prominent rock materials properties, an increase in Young's modulus could lead to a more significant elevation in thermal stress induced by wellbore cooling. Poisson's ratio, however, has an insufficient impact on the stress state in the near-wellbore region.
- Under same loading condition, fracture plugging in linear elasticity model is more effective than in poroelasticity model, regarding the decrease of SIF with same plugging position.
- Inner filer cake build-up effectively diminishes the cooling effect on fracture tip associated with fluid leak-off. But itself alone cannot protect fracture tip from initiating under high fluid pressure and low temperature.

According to the results and conclusions of this study, following recommendations can be suggested to field application of WBS while taking thermal effect into consideration:

- The effectiveness of WBS is strongly weakened as formation temperature decreases due to cold mud invasion. Plugging at fracture mouth can minimize the thermal effect on fracture tip the most. This justifies always choosing larger PSD of LCM materials when fracture is plugging dominate the effectiveness of WBS and fracture reinitiation prevention.
- Fluid leak-off rate, or lost circulation rate, significantly intensifies the negative effect of formation cooling on fracture re-initiation. Preliminary lost circulation prevention methods

are suggested before WBS implementation, especially when high fluid loss rate and a large temperature drop of formation exist simultaneously during drilling.

In this thesis, some necessary assumptions and simplification are made due to the limitation of the FEM tool, to avoid an over-complicated simulation, and to maintain a consistent topic of discussion. Several future works are suggested based on these assumptions.

1. Due to the limitation of the FEM software adopted in this study, the author assumed a sufficient rock strength, meaning fracture propagation is not allowed in any loading condition. The analysis of fracture propagation is thus limited within the study of SIF, and no relation is established to fracture pressure, which is a much more useful parameter in drilling practice. Therefore, future works are suggested to connect the simulation of stress state in near wellbore region with the actual fracture re-initiation pressure during lost circulation. The author suggests establishing the mathematical relationship between the wellbore fracture pressure and breakdown criteria of pre-existing fractures under thermal effect, as fracture toughness (or "stress intensity") in this study.
2. Extending the current work to actual fracture pressure is also beneficial to consider different rock type and more complicated loading conditions into the analysis of lost circulation under the formation cooling process.
3. The simulation in this thesis adopted input data from previous literature. Future simulations based on real operation dataset including temperature measurement are suggested to provide substantial instructions to specific drilling scenarios in practice with the concerns of the severe cooling effect of near wellbore formation.
4. This thesis only analyzed a few important factors in ANOVA test. More parametric studies on fracture geometry, in situ stress state, and thermal properties of related materials are

suggested in future simulations and subsequent ANOVA analysis to delineate the importance of different factors on induced thermal stress and possible fracture propagation under thermal effect.

5. More experimental works are encouraged to explore the possible range of fluid thermal properties of mud with different compositions when considering the heat exchange between circulating fluid and formation in near wellbore region. This will be crucial to the calculation of temperature drop and thus induced thermal stresses in near wellbore region.

References

Anderson, T. L. (1995). *Fracture Mechanics: Fundamentals and Applications*, Second edition. CRC Publications, 49-51.

Bhushan, A. et al. (2015). Finite element evaluation of j-integral in 3d for nuclear grade graphite using COMSOL-Multiphysics. 2015 COMSOL Conference.

Chang, J. H. and Becker, E. B. (1992) Finite element calculation of energy release Rate for 2-d rubbery material problems with Non-conservative crack surface tractions. *International journal for numerical methods in engineering*. 33: 907-927

Chen, G., and Ewy, R. T. (2005). "Thermoporoelastic Effect on Wellbore Stability". *SPE Journal.*10: 121-129. https://doi.org/10.2118/89039-PA.

Chen, Y., Yu, M., Takach, N., Shi, Z., and Gao, C. (2015). Hidden Impact of Mud Loss on Wellbore State of Stresses Disclosed by Thermal-Poro-Elastic Modeling. 49th U.S. Rock Mechanics/Geomechanics Symposium.

Chen, Y., Yu, M., Miska, S., Ozbayoglu, E., Zhou, and Al-Khanferi, Nasser. (2017) "Fluid flow and Heat Transfer Modeling in the Event of Lost Circulation and Its Application in Locating Loss Zones. *Journal of Petroleum Science and Engineering*. 148: 1-9, https://doi.org/10.1016/j.petrol.2016.08.030.

Clifton, R. J., Simonsen, E. R., Jones, A. H., and Green, S. J. (1976). Determination of the critical stress intensity factor, KIC, from internally pressurized thick-walled vessels. 16: 233-238.

COMSOL, *Subsurface Flow Module User Guide (Darcy's flow)*

COMSOL, *CFD Module User Guide (Heat Transfer and Non-isothermal flow)*

Dokhani, V., Ma, Y., and Yu, M. (2016). Determination of equivalent circulating density of drilling fluids in deepwater drilling. *Journal of Natural Gas Science and Engineering*. 34: 1096-1105, https://doi.org/10.1016/j.jngse.2016.08.009.

Feng, Y., Arlanoglu, C., Podnos, E., Becker, E., & Gray, K. E. (2015). Finite-Element Studies of Hoop-Stress Enhancement for Wellbore Strengthening. *Society of Petroleum Engineers,* https://doi.org/10.2118/168001-PA

Feng, Y., Gray, K. E. (2016) a. A fracture-mechanics-based model for wellbore strengthening Applications. *Journal of Natural Gas Science and Engineering*. 29: 392-400. https://doi.org/10.1016/j.jngse.2016.01.028.

Feng, Y., Gray, K.E. (2016) b. A parametric study for wellbore strengthening,"Journal of *Natural Gas Science and Engineering*, 30: 350-363, https://doi.org/10.1016/j.jngse.2016.02.045.

Feng, Y., Gray, K.E., 2017, Review of fundamental studies on lost circulation and wellbore Strengthening. *Journal of Petroleum Science and Engineering*. 152: 511-522. https://doi.org/10.1016/j.petrol.2017.01.052.

Fjær, E. and Holt, R.M. (2008). Stresses around boreholes - Borehole failure criteria. *Petroleum Related Rock mechanics*. Elsevier. 4: 135-174

Gonzalez, M. E., Bloys, J. B., Lofton, J. E., Pepin, G. P., Schmidt, J. H., Naquin, C. J., Laursen, P. E. (2004). Increasing Effective Fracture Gradients by Managing Wellbore Temperatures. IADC/SPE Drilling Conference.

Guo, Q., Feng, Y. Z., Jin, Z.H. (2011). Fracture Aperture for Wellbore Strengthening Applications. 45th U.S. Rock Mechanics / Geomechanics Symposium. American Rock Mechanics Association.

Guo, T., Li, Y., et al., (2017). Evaluation of Acid Fracturing Treatments in Shale Formation. *Energy & Fuels* 31(10): 10479-10489. https://doi.org/10.1021/acs.energyfuels.7b01398.

Hettema, M. H. H., Bostram, B., Lund, T. (2004). Analysis of Lost Circulation during Drilling in Cooled Formations. Society of Petroleum Engineers, SPE Annual Technical Conference and Exhibition.

Holzbecher E., 2013, Poroelasticity Benchmarking for FEM on Analytical Solutions, COMSOL Conference.

Hoxha, B. B., Incedalip, O., Vajargah, A. K., Hale, A., & Oort, E. van. (2016). Thermal Wellbore Strengthening: System Design, Testing, and Modeling. SPE Deepwater Drilling and Completions Conference. https://doi.org/10.2118/180315-MS.

Ito, T., Zoback, M.D., Peska, P. (2001). Utilization of Mud Weights in Excess of the Least Principal Stress to Stabilize Wellbores: Theory and Practical Examples. *SPE Drilling and Completion*. 16: 221–229. https://doi.org/10.2118/57007-PA.

Kabir, C. S., Hasan, A. R., Kouba, G. E., & Ameen, M. (1996). Determining Circulating Fluid Temperature in Drilling, Workover, and Well Control Operations. *Society of Petroleum Engineers*. https://doi.org/10.2118/24581-PA.

Knappett, J. A., and Craig, R. F. (2012). *Soil mechanics*. Eighth edition. CRC Press. 78-79.

Maury, V. and Guenot, A. (1995). Practical advantages of mud cooling systems for drilling. *SPE Drilling and Completion*, 42-48.

Morita, N., and Fuh, G.-F. (2011). Parametric Analysis of Wellbore Strengthening Methods from Basic Rock mechanics. *Society of Petroleum Engineers*. https://doi.org/10.2118/145765-MS.

Mehrabian, A., Jamison, D. E., & Teodorescu, S. G. (2015). Geomechanics of Lost-Circulation Events and Wellbore-Strengthening Operations. *SPE Drilling & Completion*. 20(06): 1305-1316.

Nguyen, D. A., Miska, S. Z., Yu, M., & Saasen, A. (2010). Modeling Thermal Effects on Wellbore Stability. Society of Petroleum Engineers conference. https://doi.org/10.2118/133428-MS.

Pepin, G., Gonzalez, M., Bloys, J. B., Lofton, J., Schmidt, J., Naquin, C., and Ellis, S. (2004). "Effect of Drilling Fluid Temperature on Fracture Gradient: Field Measurements And Model Predictions". American Rock Mechanics Association, the 6th North America Rock Mechanics Symposium (NARMS).

Perkins, T.K. and Gonzalez, J.A. (1984). Changes in Earth Stresses around a Wellbore Caused by Radial Symmetrical Pressure and Temperature Gradients. *Society of Petroleum Engineers Journal*. 24(02). https://doi.org/10.2118/10080-PA.

Perkins, T. K., & Gonzalez, J. A. (1985). The Effect of Thermoelastic Stresses on Injection Well Fracturing. *Society of Petroleum Engineers Journal*. 25(01): 78-88. https://doi.org/10.2118/11332-PA.

Rinne, M., Shen, B., Stephansson, O. (2012). Fracture Propagation from Mechanical, Thermal and Hydraulic loadings. *Harmonising Rock Engineering and the Environment*, Qian & Zhou (eds) Taylor & Francis Group, London. 511-515.

Rice,J. R. (1968). A Path Independent Integral and the Approximate Analysis of Strain Concentration by Notches and Cracks. *Journal of Applied Mechanics*. 35: 379-386.

Salehi, Sale., and Nygaard, R. (2011). Evaluation of New Drilling Approach for Widening Operational Window: Implications for Wellbore Strengthening. SPE Production and Operations Symposium. https://doi.org/10.2118/140753-MS.

Salehi, S. (2012). Numerical simulations of fracture propagation and sealing: implications for wellbore strengthening. Doctoral Dissertations. Missouri University of Science and Technology.

Smith, M., B. and Montgomery, Carl. (2015) *Hydraulic Fracturing*. CRC Press. 112-114.

Tang, L., & Luo, P. (1998). The Effect of the Thermal Stress on Wellbore Stability. SPE India Oil and Gas Conference and Exhibition. https://doi.org/10.2118/39505-MS.

Tada, H., Paris, P.C., Irwin, G.R. (1985). *The Stress Analysis of Cracks Handbook*. Paris Productions & (Del Research Corp.).

Van Oort, E., Friedheim, J. E., Pierce, T., & Lee, J. (2011). Avoiding Losses in Depleted and Weak Zones by Constantly Strengthening Wellbores. *SPE Drilling & Completion*.

26(04). https://doi.org/10.2118/125093-PA.

Van Oort, E., and Razavi, O. S. (2014). Wellbore Strengthening and Casing Smear: The Common Underlying Mechanism. IADC/SPE Drilling Conference and Exhibition. https://doi.org/10.2118/168041-MS

Yan, C., Deng, J., Li, D., Chen, Z., Hu, L., Li, Y., (2014), Borehole Stability in High-Temperature Formations, *Rock Mechanics and Rock Engineering*. 47(6): 2199–2209, https://doi.org/10.1007/s00603-013-0496-2.

Rui, Z., Lu, J., Zhang, Z., Guo, R., Ling, K., Zhang, R. and Patil, S. (2017). A quantitative oil and gas reservoir evaluation system for development. *Journal of Natural Gas Science and Engineering*. 42: 31-39. https://doi.org/10.1016/j.jngse.2017.02.026.

Zhong, R., Miska, S., and Yu, M. (2017). Parametric study of controllable parameters in fracture-based wellbore strengthening. *Journal of Natural Gas Science and Engineering*. 43: 13-21. https://doi.org/10.1016/j.jngse.2017.03.018.

Zhong, R., Miska, S. and Yu, M. (2017). Modeling of near-wellbore fracturing for wellbore strengthening. *Journal of Natural Gas Science and Engineering*. 38: 475-484 https://doi.org/10.1016/j.jngse.2017.01.009.

Zhou, X., Aydin, A., Liu, F. and Pollard, D. D. (2010). Numerical Modeling of Secondary Thermal Fractures in Hot Dry Geothermal Reservoirs, 35th Workshop on Geothermal Reservoir Engineering, Stanford University.

Vita

Ze Wang is an international student from Inner Mongolia Autonomous Region in China. Ze holds his B.S. degree in petroleum engineering from China University of Petroleum (Beijing). He began his study at Louisiana State University in Spring of 2016. Ze then worked as a research assistant from August of 2016 in the research group funded by Professor Yuanhang Chen until the end of his Master's study.